**Article**

# The *Il6* -39 kb enhancer containing clustered GATA2- and PU.1-binding sites is essential for *Il6* expression in murine mast cells



Shin'ya Ohmori, Jun Takai, Satoshi Uemura, Akihito Otsuki, Tetsuya Mori, Kinuko Ohneda, Takashi Moriguchi

moriguchi@tohoku-mpu.ac.jp

**Highlights**

GATA2- and PU.1-binding peaks are closely located in distal enhancers of cytokine genes

GATA2 and PU.1 play crucial roles in promoting LPS-mediated cytokine induction

The *Il6* -39 kb enhancer containing GATA2 and PU.1 motifs are crucial for *Il6* induction

GATA2 inhibitor exerts anti-inflammatory effects via reducing cytokine induction

# iScience

## Article

# The *Il6* -39 kb enhancer containing clustered GATA2- and PU.1-binding sites is essential for *Il6* expression in murine mast cells

Shin'ya Ohmori,[1] Jun Takai,[2] Satoshi Uemura,[2] Akihito Otsuki,[3] Tetsuya Mori,[1] Kinuko Ohneda,[3] and Takashi Moriguchi[2,4,*]

## SUMMARY

**Mast cells serve as a first-line defense of innate immunity. Interleukin-6 (IL-6) induced by bacterial lipopolysaccharide (LPS) in mast cells plays a crucial role in antibacterial protection. The zinc finger transcription factor GATA2 cooperatively functions with the ETS family transcription factor PU.1 in multiple mast cell activities. However, the regulatory landscape directed by GATA2 and PU.1 under inflammation remains elusive. We herein showed that a large proportion of GATA2-binding peaks were closely located with PU.1-binding peaks in distal *cis*-regulatory regions of inflammatory cytokine genes in mast cells. Notably, GATA2 and PU.1 played crucial roles in promoting LPS-mediated inflammatory cytokine production. Genetic ablation of GATA2-PU.1-clustered binding sites at the *Il6* -39 kb region revealed its central role in LPS-induced *Il6* expression in mast cells. We demonstrate a novel collaborative activity of GATA2 and PU.1 in cytokine induction upon inflammatory stimuli via the GATA2-PU.1 overlapping sites in the distal *cis*-regulatory regions.**

## INTRODUCTION

Mast cells are tissue-resident immune cells located in mucosal and subcutaneous tissues throughout the body. Numerous studies have established that mast cells function as critical effector cells in allergic inflammation (Bischoff, 2007; Mukai et al., 2016). Allergen–immunoglobulin E (IgE) complexes bind to the high-affinity IgE receptor (FcεRI) on the mast cell surface, which promotes immediate allergic reactions via the release of inflammatory mediators, including histamine, serotonin, and mast-cell-specific proteases. These mast-cell-derived products promote tissue inflammation by recruiting other inflammatory cells, such as monocytes, neutrophils, and T cells (Cardamone et al., 2016). Mast cells also constitute the first line of defense against microbial pathogens. Mast cells have been reported to play essential roles in resistance to bacterial infections by producing inflammatory cytokines and promoting the recruitment of various immune cells (Abraham and St John, 2010; Rodewald and Feyerabend, 2012). A recent report demonstrated that mast-cell-deficient mice exhibited impaired bacterial clearance and delayed healing of infectious skin wounds (Zimmermann et al., 2019). Subsequent closer immunological analyses demonstrated that the antibacterial defense and wound healing largely depended on interleukin-6 (IL-6) secretion from the infiltrating mast cells, which supports the importance of mast-cell-derived IL-6 in the antimicrobial immune response (Zimmermann et al., 2019).

The proinflammatory cytokine IL-6 was initially characterized as an inducer of B-cell growth and antibody production (Hirano et al., 1985; reviewed in Kishimoto, 2010), and it plays a critical role in the defense against pathogenic microorganisms. IL-6-deficient mice exhibit increased susceptibility to multiple infectious diseases (Kopf et al., 1994; Ladel et al., 1997; Dienz et al., 2012). In humans, IL-6 aberrations underlie the etiology of various inflammatory disorders, e.g., rheumatoid arthritis and cytokine release syndrome (Tanaka et al., 2014). Neutralizing anti-IL-6 or anti-IL-6 receptor (IL-6R) monoclonal antibodies are used globally to treat these inflammatory diseases. However, these therapeutic agents are often associated with an increased incidence of serious infections as unwanted adverse effects, presumably due to compromised immune responses (Rose-John et al., 2017).

Mechanisms that regulate IL-6 expression have also been intensively investigated because modulation of IL-6 expression has potential therapeutic utility (Medzhitov and Horng, 2009; Glass and Saijo, 2010; Smale,

[1]Department of Pharmacy, Faculty of Pharmacy, Takasaki University of Health and Welfare, Takasaki, Japan

[2]Division of Medical Biochemistry, Tohoku Medical Pharmaceutical University, Sendai, Japan

[3]Division of Genomics and Disease Prevention, Tohoku Medical Megabank Organization, Tohoku University, Sendai, Japan

[4]Lead contact

*Correspondence: moriguchi@tohoku-mpu.ac.jp

https://doi.org/10.1016/j.isci.2022.104942

2010). The expression of *Il6* and other cytokine genes is strongly induced by microbial products, including lipopolysaccharide (LPS), which are sensed by Toll-like receptors (TLRs) in the innate immune system (Barton and Medzhitov, 2003). LPS is the principal constituent of the Gram-negative bacterial outer membrane and activates TLR4 on mast cells to promote the translocation of nuclear factor-kappa B (NF-κB) to the nucleus and accelerate cytokine production without degranulation (Supajatura et al., 2001; Krystel-Whittemore et al., 2016). Considering the crucial function of mast-cell-derived IL-6 in host immune defense, elucidation of the regulatory mechanism controlling *Il6* gene expression in mast cells will crucially advance our understanding of the innate immune system.

The zinc finger transcription factor GATA2 plays an essential role in hematopoietic development via physical and genetic interactions with numerous other nuclear proteins (Doré and Crispino, 2011; Wu et al., 2014), including the E-twenty-six (ETS)-domain transcription factor PU.1(encoded by the *Spi1* gene), which governs the differentiation of myeloid lineage cells. GATA2 and PU.1 are expressed in mast cells and play roles in their differentiation and function (Li et al., 2015; Ohmori et al., 2015; Walsh et al., 2002). Many studies have shown that GATA factors and PU.1 reciprocally inhibit their respective activities via multiple mechanisms (Rekhtman et al., 1999; Zhang et al., 1999, 2000; Nerlov et al., 2000; Arinobu et al., 2007; Burda et al., 2016). However, recent studies demonstrated that these factors cooperatively activate the expression of several genes in mast cells, including *Il1rl1*, which encodes a transmembrane receptor for IL33, and *Ms4a2*, which encodes the β-chain of the high-affinity IgE receptor (FcεRI) (Baba et al., 2012; Ohmori et al., 2019). We recently demonstrated that the LPS-mediated induction of multiple peritoneal cytokines was under an intense regulatory influence of GATA2 (Takai et al., 2021). Heterozygous GATA2 mutant mice showed attenuated inflammatory responses with reduced levels of multiple cytokines (Takai et al., 2021). These results suggest that GATA2 collaborates with PU.1 in the regulatory processes of inflammation-related genes in immune cells.

The present study delineated genome-wide GATA2 and PU.1 binding profiles upon LPS stimulation using ChIP-seq analysis in a murine mast cell line, MEDMC-BRC6. We found that a large proportion of GATA2-binding peaks closely localized with PU.1-binding peaks. These GATA2-PU.1 overlapping peaks were preferentially located in *cis*-regulatory regions of multiple cytokine gene loci irrespective of the LPS stimulus. We demonstrated that the 5′ 39 kb distal regulatory element in the *Il6* locus carried GATA2-PU.1-clustered binding sites and played a crucial role in stimulation-induced *Il6* expression in mast cells.

## RESULTS

### GATA2 constitutively binds to the enhancers of various cytokine loci

We aimed to elucidate where and how GATA2 bound to chromatin and controlled gene expression during inflammatory processes. To this end, we conducted ChIP-seq analysis to address GATA2-binding sites in mast cells upon inflammatory stimuli. We used the murine mast cell line MEDMC-BRC6 (BRC6). BRC6 cells were generated from C57BL/6-derived ES cells cultured on OP9 feeder cells supplemented with stem cell factor (SCF) and IL-3 cytokines (Hiroyama et al., 2008). BRC6 cells express FcεRI and SCF receptor (c-Kit) and thereby respond to IgE/antigen stimulation and SCF signaling as normal mast cells (Shibagaki et al., 2017). Furthermore, BRC6 cells produce numerous inflammatory cytokines upon LPS stimulation (Shibagaki et al., 2017). We prepared GATA2-ChIPed samples under basal and LPS-stimulated conditions 2 h post-LPS treatment to observe LPS-induced epigenomic and transcriptional changes (Figure 1A). We profiled H3K27 acetylation (H3K27ac) in the same crosslinked samples to identify active enhancers (Rada-Iglesias et al., 2011). The total GATA2 peaks amounted to 3,258, commonly detected in untreated and LPS-treated BRC6 cells (Figure 1B). There were 646 GATA2 peaks associated with H3K27ac accumulation; thus, 20% of the total GATA2 peaks (646/3258) resided in the H3K27ac-positive enhancer regions (Figure 1B).

We previously reported that a cohort of peritoneal cytokines was decreased in LPS-treated *Gata2* heterozygous mutant mice (Takai et al., 2021). Notably, many of the gene loci of these cytokines, including *Il4*, *Il13*, and *Tnf*, were enriched in the 646 GATA2 binding enhancer peaks. The Integrated Genomics Viewer (IGV) track data showed that these cytokine gene loci were associated with GATA2 binding regardless of LPS treatment (Figure 2). Consistently, H3K27ac also constitutively accumulated at these loci irrespective of LPS stimulation (Figure 2). These results indicated that GATA2 was constitutively bound to the *cis*-regulatory regions of various cytokine gene loci regardless of the inflammatory stimulus.

**A**

No treatment

2h LPS stimulation

BRC6 cells

ChIP-seq with αGATA2, αPU.1, αH3K27ac

Peak calling with MACS2

**B**

GATA2-PU.1

GATA2-only

| 1789 | 823 | 19995 | PU.1-only |

| 278 | 368 | 4072 |

15583
H3K27ac

**C**

### Homer *de novo* Motif Enrichment (GATA2+ H3K27ac+ 646 sites)

| Rank | Consensus sequence | TF | *P*-value |
|------|-------------------|------|-----------|
| 1 | GGCCAGATAAC (logo) | GATA | $1e^{-980}$ |
| 2 | AACCAGGAAGT (logo) | ETS | $1e^{-200}$ |
| 3 | TTGTGGTTTG (logo) | RUNX | $1e^{-199}$ |
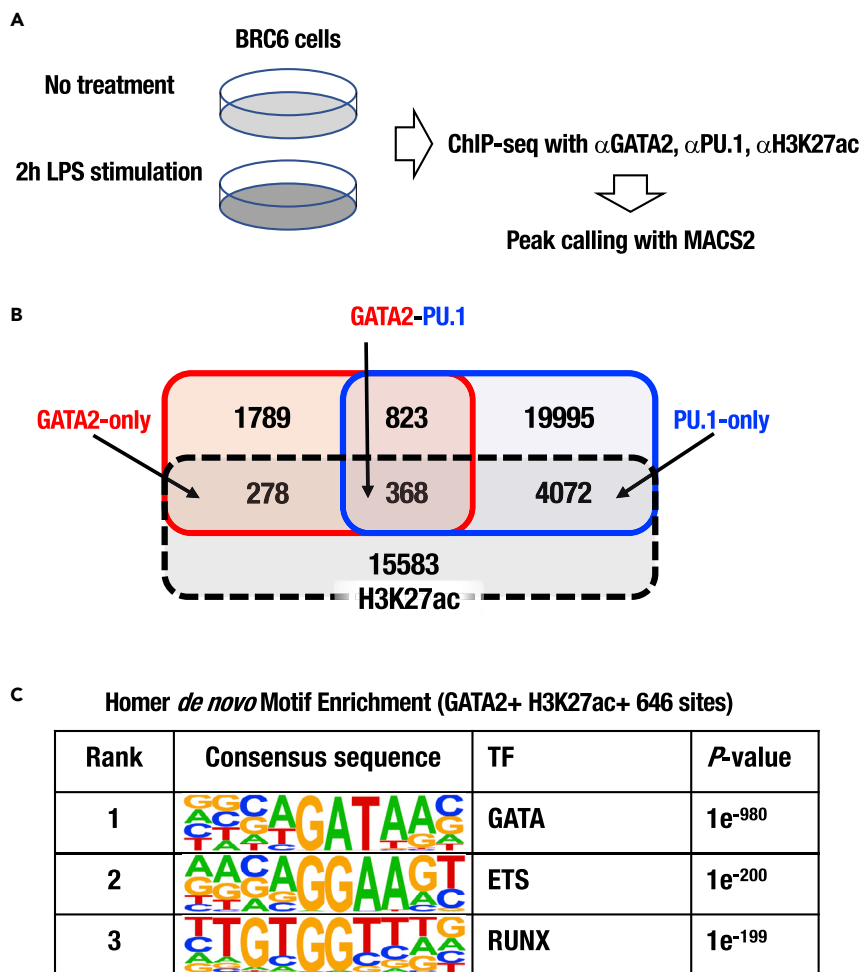
**Figure 1. ChIP-Seq profiles of GATA2, PU.1, and H3K27ac in BRC6 mast cells**

(A) BRC6 cells with and without LPS stimulation (1 μg/mL for 2 h) were subjected to ChIP-seq analysis using GATA2, PU.1, and H3K27ac antibodies.

(B) Venn diagram generated by Pybedtools depicting GATA2, PU.1, and H3K27ac peaks commonly detected in the untreated and LPS-treated BRC6 cells.

(C) Motif analysis in the GATA2 and H3K27ac overlapping peaks (646 peaks). The top 3 ranked transcription factor family motifs are shown with their p values. Note that ETS and RUNX motifs are enriched near the GATA2-binding peaks. Motif enrichment was calculated with HOMER software applying cumulative hypergeometric distribution adjusted for multiple testing with the Benjamini–Hochberg method (see STAR Methods).

## More than half of the GATA2-binding peaks are overlapped with the PU.1-binding peaks in BRC6 mast cells

Motif analysis of the 646 GATA2 peaks showed enrichment of GATA transcription factors followed by ETS domain transcription factors and runt domain transcription factors (RUNX) (Figure 1C). Because the ETS family transcription factor PU.1 functions with GATA2 in mast cells in several contexts (Ohmori et al., 2019; Baba et al., 2012), we delineated the genome-wide binding profile of PU.1 using ChIP-seq in the same LPS-treated and untreated BRC6 cell samples. We identified 25,258 PU.1-binding peaks that commonly arose in the untreated and LPS-treated cells (Figure 1B). Among them, 4,440 peaks were associated with H3K27ac accumulation (Figure 1B). We searched for overlap between the 646 GATA2 and 4,440 PU.1 enhancer peaks (H3K27ac$^+$) using Pybedtools (https://daler.github.io/pybedtools/) and identified 368 GATA2-PU.1-overlapping peaks (Figure 1B). This result indicates that more than half of the GATA2 peaks overlapped with PU.1 peaks in the H3K27ac$^+$ active *cis*-regulatory regions in BRC6 mast cells. We referred to the other 278 peaks that bound only GATA2 as GATA2-only peaks (Figure 1B). The 4,072 peaks to which
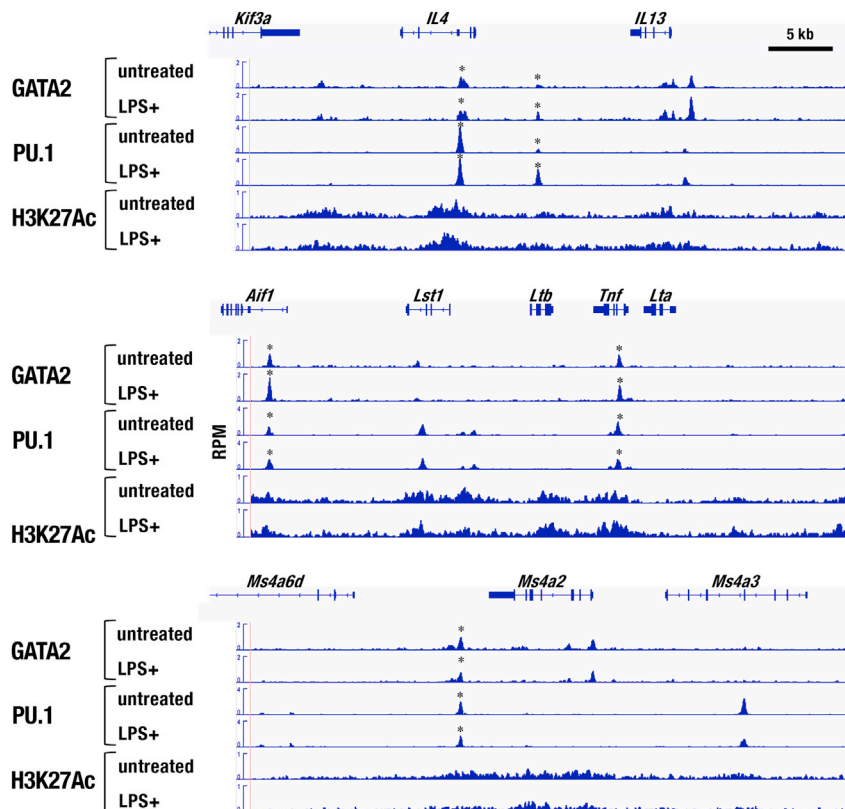
**Figure 2. GATA2 and PU.1 concomitantly bind to the distal regulatory regions of inflammatory cytokine genes**
Representative Integrative Genomics Viewer (IGV) track data showing the loci that carry GATA2-PU1 overlapping peaks in
BRC6 cells (asterisks). GATA2 and PU.1 bind to *Il4*, *Il13*, *Tnf*, and *Ms4a2* loci regardless of LPS treatment. Note that
H3K27ac densely accumulates around the GATA2-PU1 peaks. The numbers of reads in RPM (reads per million mapped
reads) are shown on the y axis.

only PU.1 bound were designated as PU.1-only peaks (Figure 1B). We subjected these distinct classes of
peaks to subsequent bioinformatics analysis.

### The genes carrying GATA2-PU.1 peaks enrich ontologies related to the immune response

To gain insight into the biological significance of genes carrying the three classes of peaks (i.e., GATA2-
only, GATA2-PU.1, and PU.1-only peaks), we performed ontology pathway analyses using GREAT
(Genomic Regions Enrichment of Annotations Tool) (http://great.stanford.edu/public/html/). We found
that genes containing GATA2/PU.1 peaks were predominantly enriched in inflammation-related ontol-
ogies, such as the immune response and cytokine production (highlighted in Figure 3B). The representative
inflammatory cytokine loci, including *Il4*, *Il6*, *Il13*, and *Tnf*, carried GATA2-PU.1 peaks and exhibited
H3K27ac accumulation regardless of LPS treatment (Figures 2 and 4). *Ms4a2*, which is cooperatively regu-
lated by GATA2 and PU.1, harbored a GATA2-PU.1 peak at the 3′ 10.4 kb region as previously reported
(Ohmori et al., 2019) (Figure 2). The GATA2-only peaks were enriched in several ontologies, including defin-
itive hematopoiesis, myeloid cell differentiation, and positive regulation of mast cell activation, which was
anticipated from the known hematopoietic function of GATA2 (Figure 3A). The PU.1-only peaks were en-
riched in ontologies related to noncoding-RNA- and ribosomal-RNA-related processes with low probabil-
ity (Figure 3C). Notably, these three classes of peaks showed distinct patterns of genomic distributions. The
GATA2-PU1 peaks were predominantly located distally (5 ∼ 500 kb) from the transcription start sites (TSS),
whereas the proximal promoter regions harbored a relatively low number of GATA2-PU1 peaks (Figure 3E).
The GATA2-only peaks were evenly distributed from the promoter to the distal regions (<500 kb) (Fig-
ure 3D). The PU.1-only peaks primarily resided in the promoter regions (<5 kb) (Figure 3F). These results
indicate that the GATA2-PU.1 peaks tend to be located in the distal flanking region (5–500 kb), and genes
associated with the GATA2-PU.1 peaks are likely involved in immune-system-related biological pathways.

## Gene Ontology analysis
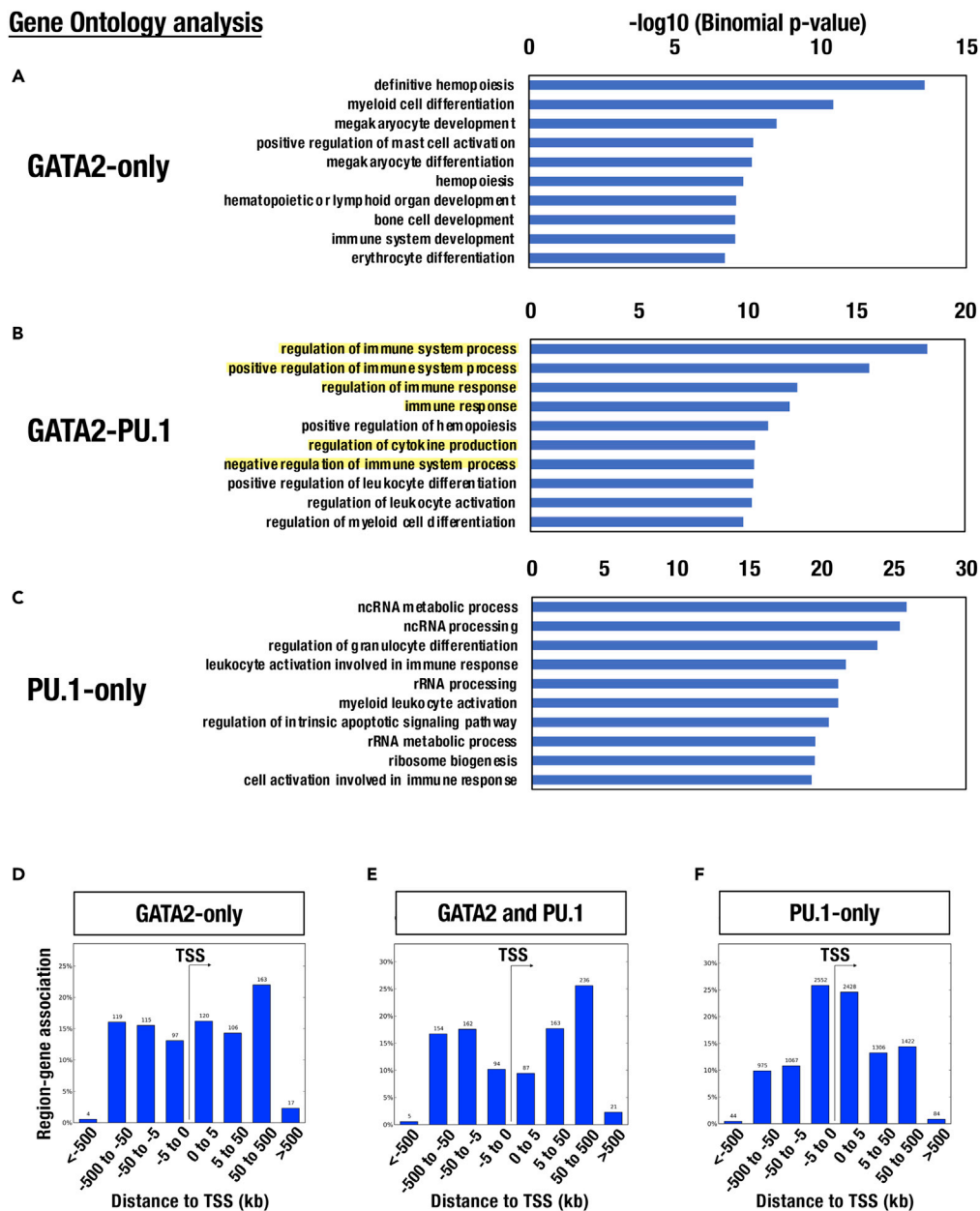


**Figure 3. Distinct gene ontology (GO) biological terms associated with the GATA2-only peaks, GATA2-PU.1 peaks, and PU.1-only peaks**

Terms including immune system processes and immune response are predominantly enriched in the GATA2-PU.1 peaks (highlighted in yellow) (B). GATA2-only-peaks-enriched ontologies included definitive hematopoiesis, myeloid cell differentiation, and positive regulation of mast cell activation (A). The PU.1-only-peaks-enriched ontologies related to ncRNA- and rRNA-related processes with low probability (C). Genomic distribution of the GATA2-only (D), GATA2-PU.1 (E), and PU.1-only (F) peaks in BRC6 cells.

(E) The GATA2-PU1 peaks were predominantly located in the distal regions (5 ∼ 500 kb) from the transcription start sites (TSS).

(D) The GATA2-only sites tended to be evenly distributed from promoter-proximal to the distal regions (>500 kb).

(F) The PU.1-only sites were mainly located in the promoter-proximal region (<5 kb). All GO analyses were conducted using the Genomic Regions Enrichment of Annotations Tool (GREAT) online software (see STAR Methods).
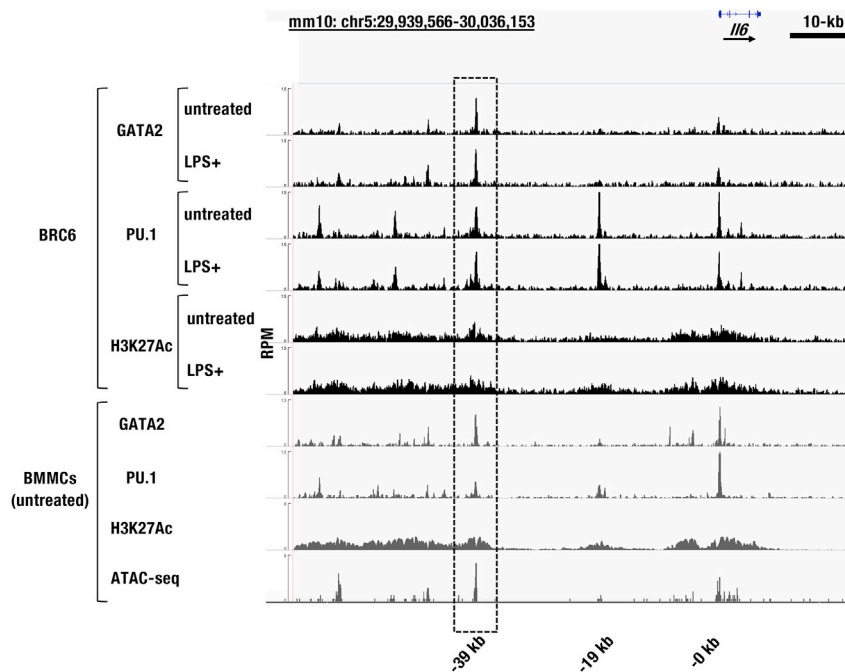
**Figure 4. GATA2-, PU.1-, and H3K27ac-binding peaks in the mouse *Il6* locus encompassing the 5′ 80 kb to 3′ 35 kb distal flanking sequences**

Note the robust GATA2- and PU.1-binding peaks at the 5′ 39 kb region in BRC6 cells and BMMCs with and without LPS stimulation (dotted rectangles). GATA2, PU.1, and H3K27ac ChIP-seq data and ATAC-seq data in the untreated BMMCs were obtained from the NCBI Sequence Read Archive (SRA) database (see STAR Methods).

### GATA2-PU.1 peaks at the 5′ 39 kb region in the *Il6* locus exhibit active histone marks

IL-6 secreted from infiltrating mast cells plays a role in the antimicrobial innate immune response (Zimmermann et al., 2019). Therefore, we focused on the regulatory mechanism of *Il6* gene expression in mast cells. A series of analyses demonstrated that several transcription factors, including IRF, AP-1, C/EBP, SP1, and NF-κB, responded to many types of stimuli and activated *Il6* gene expression via regulatory sequences in the proximal promoter region (reviewed in Medzhitov and Horng, 2009). Meanwhile, evolutionarily conserved putative *cis*-regulatory elements are broadly distributed from approximately 165 kb upstream to 35 kb downstream of the human *IL6* gene (Samuel et al., 2008). Indeed, we demonstrated that 176 kb human *IL6* BAC (bacterial artificial chromosome) (5′ 90 kb and 3′ 86 kb to promoter)-driven luciferase transgenic mice faithfully recapitulated the endogenous mouse *Il6* gene expression pattern in multiple tissues *in vivo*, which suggests that a comprehensive set of *cis*-regulatory regions are contained in the 176 kb human *IL6* BAC (Hayashi et al., 2015). To examine novel distal regulatory elements, we searched for GATA2-PU.1 peaks in a broad range of up- and downstream regions of the mouse *Il6* locus. We found that several robust GATA2-PU.1 peaks were distributed around the promoter and the 5′ distal flanking regions of the mouse *Il6* locus in BRC6 cells, which occurred regardless of LPS treatment (Figure 4). These GATA2-PU.1 peaks were also detected in unstimulated bone-marrow-derived mast cells (BMMCs) in ChIP-seq data from the public database (Figure 4). The most prominent GATA2-PU.1 peak was located at the 5′ 39 kb region (see the dotted rectangle in Figure 4). H3K27ac signals also accumulated around the -39 kb peak in BRC6 cells and BMMCs, suggesting its potent enhancer activity. The assay for transposase-accessible chromatin (ATAC)-seq results in the BMMCs showed increased chromatin accessibility around the -39 kb region (bottom row in Figure 4). These results suggest that the GATA2-PU.1 peak at the *Il6*-39 kb region functions as an enhancer element in mast cells.

### GATA2 and PU.1 robustly bind to the -39 kb region of *Il6* in mast cells

To validate the ChIP-seq results, we conducted quantitative ChIP analysis (ChIP–qPCR) in BRC6 cells and BMMCs using real-time PCR with primer pairs amplifying the *Il6* -39 kb, -19 kb, promoter, and first intron regions, which showed GATA2 and/or PU.1 peaks (Figure 4). We detected the most robust GATA2
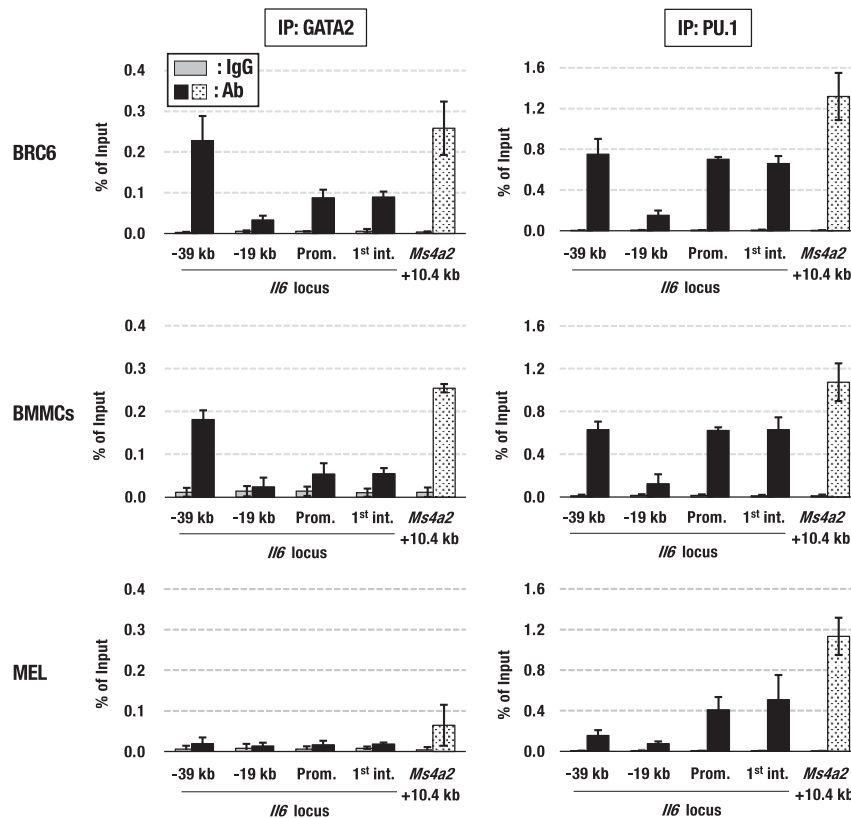
**Figure 5. Quantitative chromatin immunoprecipitation (ChIP–qPCR) analysis of GATA2 and PU.1 binding at the *Il6* locus in BRC6, BMMCs, and MEL cells**

Note that GATA2 and PU.1 robustly bind to the -39 kb region in BMMCs and BRC6 cells but not in MEL cells. MEL cells showed only marginal GATA2 and PU.1 binding at the -39 kb region. GATA2 and PU.1 are both bound to the positive locus, i.e., the +10.4 kb region in the *Ms4a2* locus in the BMMCs, BRC6, and MEL cells, as reported (Ohmori et al., 2019).

occupancy at the -39 kb region, followed by the promoter, and the first intron regions in BRC6 cells and BMMCs, which confirmed the ChIP-seq results (Figure 5). Consistent with this GATA2 binding pattern, we detected prominent PU.1 accumulation at the -39 kb, the promoter, and first intron regions in BRC6 cells and BMMCs. ChIP–qPCR analysis showed that GATA2 and PU.1 binding at the -19 kb region was weaker than that at the other regions, which suggests lower regulatory activity. In contrast, mouse erythroleukemia (MEL) cells showed weak GATA2 and PU.1 binding at the -39 kb region, whereas PU.1 bound to the promoter and the first intron regions of the *Il6* locus to some extent in MEL cells (Figure 5). These results suggest that the *Il6* -39 kb region, where GATA2 and PU.1 robustly bind, functions as a potent enhancer element for mouse *Il6* expression in mast cells.

## GATA2 and PU.1 participate in LPS-mediated *Il6* induction

We examined whether and how GATA2 and PU.1 contributed to *Il6* mRNA expression using siRNA knockdown, which reduced *GATA2* and *PU.1* mRNA expression to 15% and 17%, respectively, in BRC6 cells (Figure 6A-a and -b). si*GATA2* knockdown expectedly diminished basal expression of *Tpsb2* (tryptase beta-2), a known GATA2 target gene in BMMCs (Figure S1) (Ohneda et al., 2019). *Ms4a2*, a direct target of both GATA2 and PU.1, was also significantly decreased by *GATA2* and/or *PU.1* knockdown (Figure S1). LPS treatment (1 μg/mL) induced *Il6* mRNA expression up to 6.5-fold 2 h after LPS treatment relative to the non-treated control level in BRC6 cells (Figure 6A-c). si*GATA2* knockdown reduced LPS-induced *Il6* expression by 50% compared with the control siRNA (p = 0.014) (Figure 6A-c). In contrast, si*PU.1* knockdown rarely reduced LPS-induced *Il6* expression (Figure 6A-c). Simultaneous *GATA2* and *PU.1* knockdown conferred a similar level of *Il6* reduction as *GATA2* single knockdown (Figure 6A-c). *Il13*, which is a known target gene of GATA2, showed a similar trend of a significant reduction by si*GATA2* (Figure 6A-d) (Li et al., 2015). Notably, si*PU.1* increased *Il13* expression, which suggests a negative regulatory influence of PU.1
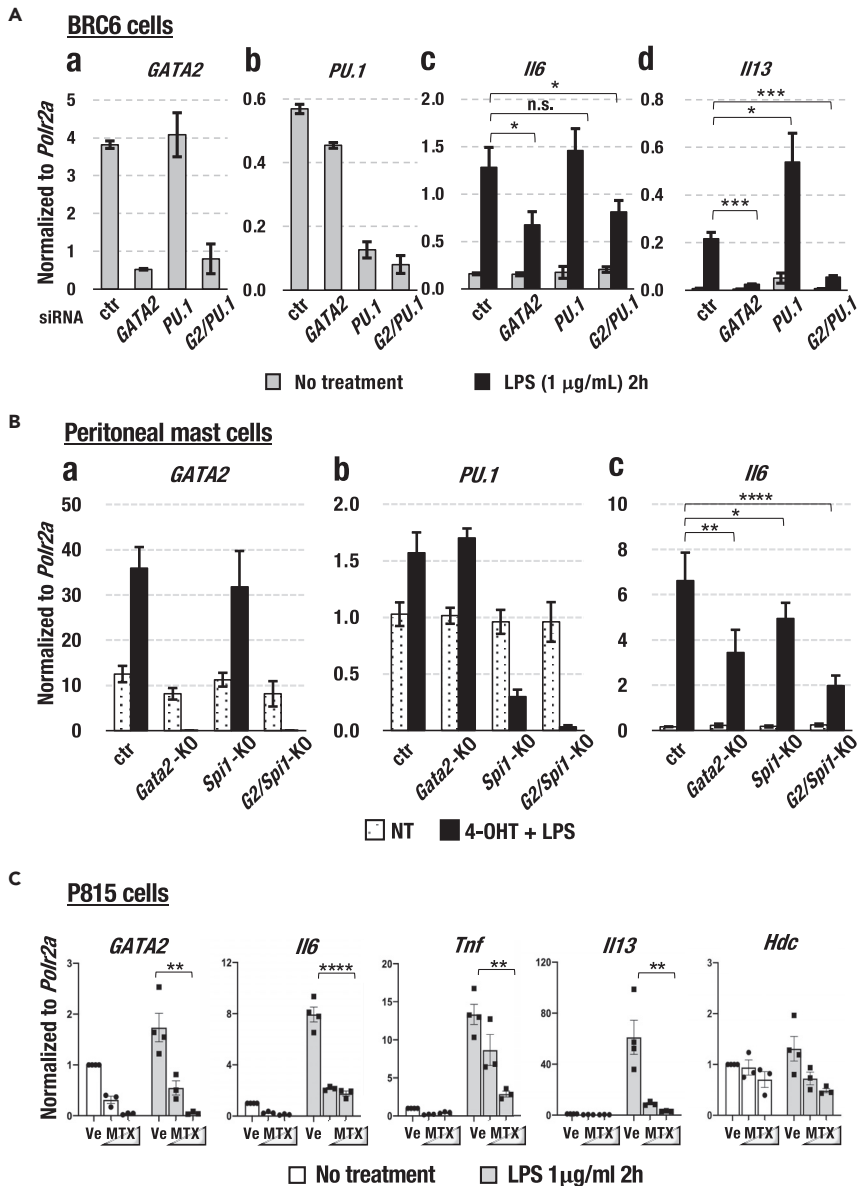
**Figure 6. GATA2 and PU.1 participate in cytokine gene regulation in BRC6 cells and peritoneal mast cells**

siRNA knockdown diminished *GATA2* and *PU.1* mRNA expression to 15% and 17%, respectively, in BRC6 cells (A-a and -b). si*GATA2* knockdown reduced LPS-induced *Il6* and *Il13* expression in the BRC6 cells (A-c and -d). *Gata2*-, *Spi1*-, or both-deficient peritoneal mast cells (PMCs) were developed from *Gata2*$^{flox/flox}$ and/or *Spi*$^{flox/flox}$ mice carrying the Rosa26-CreERT2 allele (B-a and -b). The LPS-induced *Il6* mRNA level was decreased in the *Gata2*-, *Spi1*-,or both-deficient PMCs. For Panels (A) and (B), data are presented as the mean ± SD and were analyzed by one-way ANOVA with Dunnett's post-hoc test.

(C) The GATA inhibitor, mitoxantrone (MTX), reduced *GATA2* mRNA expression levels in an MTX-dose-dependent manner (0.05 and 0.5 μM) in the P815 mastocytoma-derived cell line. Note that the basal- and LPS-induced expression of *Il6*, *Tnf*, *and Il13* was significantly diminished upon MTX administration. Ve, vehicle. Data in (C) are presented as the mean ± SEM and analyzed by one-way ANOVA with the Tukey–Kramer test. Statistically significant differences for all data are indicated by p values; *p < 0.05; **p < 0.01; ***p < 0.001; ****p < 0.0001; n.s., not significant.

(Figure 6A-d). Simultaneous *GATA2* and *PU.1* knockdown reduced *Il13* expression to a similar level as *GATA2* single knockdown, which supports the potent positive regulatory influence of GATA2 on *Il13* expression. These results indicated that GATA2 exerted a positive regulatory influence on the LPS-induced expression of a certain group of cytokines in BRC6 mast cells.

A



B **BRC6 cells**



C **BRC6 cells**



D **RAW264.7 cells**



E
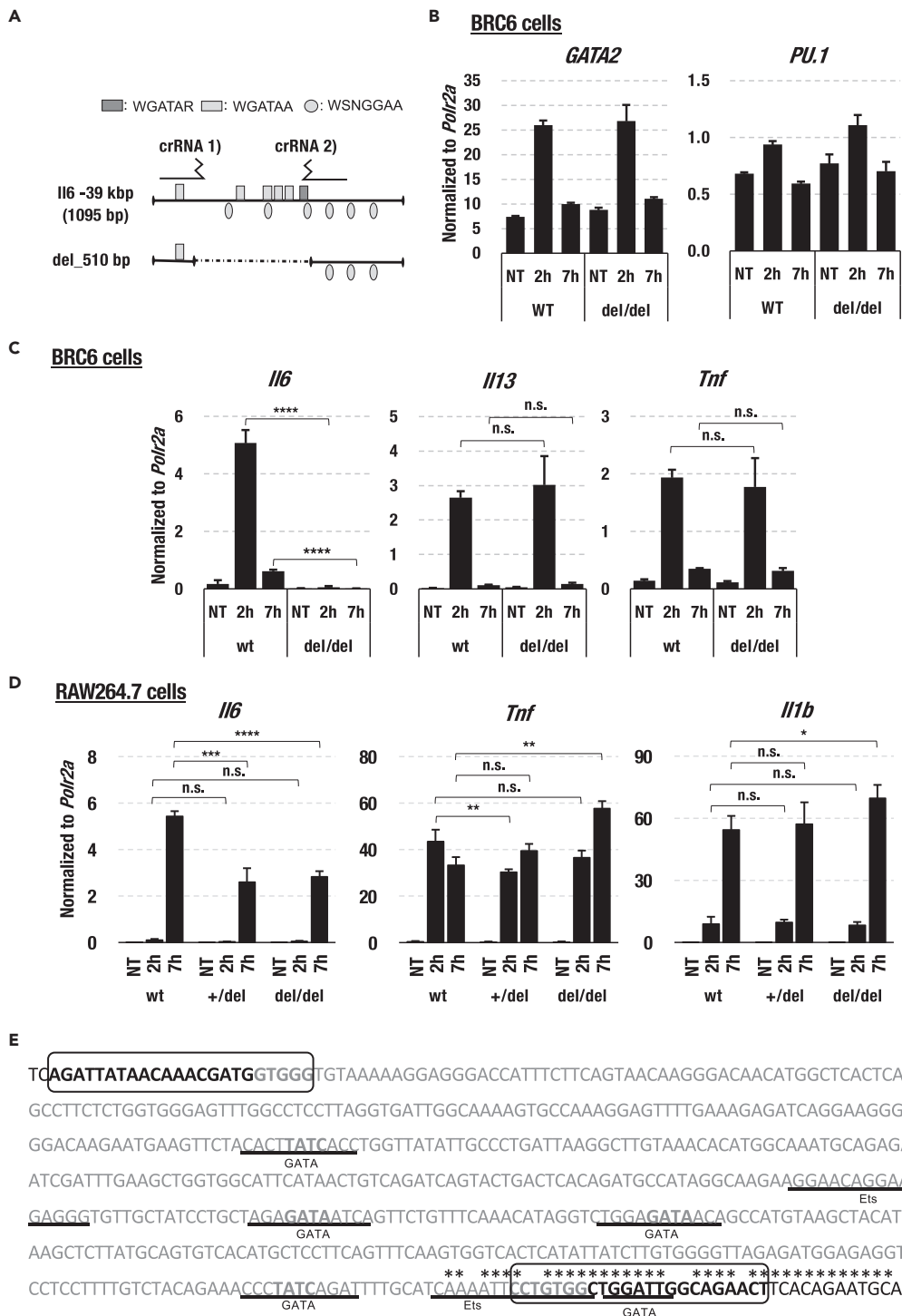


**Figure 7. CRISPR/Cas9-mediated genomic deletions of the *Il6* -39 kb enhancer reveal principal roles of the clustered PU.1- and GATA-bound regions in the BRC6 cells**

(A) Schematic diagram depicting the targeted deletion of the -39 kb region of the mouse *Il6* locus.

(B and C) Homozygous deletion of the -39 kb enhancer region significantly diminished basal-and LPS-induced *Il6* mRNA expression, whereas the expression levels of *GATA2*, *PU.1*, *Il13*, and *Tnf* were maintained.

(D) LPS-stimulated *Il6* expression was decreased to 50% in heterozygous (+/del) and homozygous (del/del) -39 kb element-deficient RAW264.7 cells. *Tnf* and *Il1b* levels were slightly increased in the del/del RAW264.7 cells at 7 h after stimulation. For panels (C) and (D), statistically significant differences compared with the wild-type control at the same

**Figure 7. *Continued***
stage are indicated; *p < 0.05; **p < 0.01; ***p < 0.001; ****p < 0.0001; n.s., not significant (one-way ANOVA with Dunnett's post-hoc test).

(E) Nucleotide sequences of the -39 kb region of the mouse *Il6* gene. Putative transcription factor binding sites were predicted by JASPAR (http://jaspar.genereg.net). Positions of CRISPR RNAs (crRNAs) are indicated by circles. Nucleotide sequences conserved in the 5' 30 kb region of human *IL6* are indicated by asterisks. Nucleotide sequences deleted by the CRISPR/Cas-9 system are in gray.

We examined these trends in peritoneal-cell-derived mast cells (PMCs), which represent tissue-resident mast cells and recapitulate the physiological relevance for inflammatory conditions *in vivo*. We prepared PMCs from *Gata2*^flox/flox or *Spi1*^flox/flox mice carrying the Rosa26-CreER^T2 allele that were treated with 4-hydroxytamoxifen (4-OHT) for 24 h to induce Cre-loxP-mediated recombination (*Gata2*-KO or *Spi1*-KO PMCs) (Ohmori et al., 2019). *Gata2*^flox/flox:*Spi1*^flox/flox:Rosa26-CreER^T2 compound double-deficient mice were also generated to prepare simultaneous *Gata2*/*Spi1*-KO PMCs. *Gata2*-KO PMCs showed a decrease in *Tpsb2* mRNA expression consistent with the results in the si*GATA2* BMC6 cells (Figure S2). *Ms4a2* mRNA was also significantly decreased in the *Gata2*-KO, *Spi1*-KO, and *Gata2*/*Spi1*-KO PMCs (Figure S2). *Il6* mRNA expression was significantly induced (more than 100-fold) in WT PMCs after 2 h of LPS treatment (Figure 6B-c). The *GATA2* mRNA expression level was slightly increased 2.5-fold 2 h after LPS treatment (Figure 6B-a). The 4-OHT treatment for 24 h almost completely diminished *GATA2* mRNA expression in the *Gata2*-KO PMCs (Figure 6B-a). Consistent with this *GATA2* reduction, the LPS-induced *Il6* level was decreased to 50% of the levels observed in WT PMCs (Figure 6B-c). *PU.1* mRNA increased 1.6-fold after LPS treatment in WT PMCs (Figure 6B-b). *PU.1* mRNA after LPS treatment decreased to 20% in *Spi1*-KO PMCs compared with LPS-treated WT PMCs (Figure 6B-b). Consequently, LPS-induced *Il6* mRNA expression was slightly but statistically significantly reduced to 74.4% in *Spi1*-KO PMCs compared with the control (Figure 6B-c). *Gata2*- and *Spi1*-double KO more profoundly reduced LPS-induced *Il6* expression to 28% compared with the WT control (Figure 6B-c). These results demonstrated that GATA2 and PU.1 collaboratively played a role in LPS-induced *Il6* mRNA expression in peritoneal mouse mast cells.

## GATA2 participates in LPS-induced cytokine gene regulation in the P815 mast cell line

We examined whether GATA2 participated in inflammatory cytokine gene regulation in another type of mast cell line, murine mastocytoma-derived P815 cells, in which GATA2 regulates a series of mast-cell-affiliated genes (Zon et al., 1991; Lunderius et al., 2000). LPS treatment (1 μg/mL for 2 h) induced the mRNA expression of *Il6*, *Il13*, and *Tnf* in P815 cells (Figure 6C). LPS treatment slightly increased *GATA2* mRNA expression by 1.74-fold, as observed in BRC6 cells and PMCs (Figure 6C). To address the loss of GATA2 function, we used an anthraquinone derivative that was identified as a GATA2-specific inhibitor, mitoxantrone (MTX) (Yu et al., 2017; Kaneko et al., 2017). MTX significantly reduced *GATA2* mRNA expression in a dose-dependent manner, as previously reported (Figure 6C). MTX treatment reduced the steady-state and induced expression of *Il6*, *Tnf*, and *Il13*, suggesting that GATA2 participates in LPS-mediated inducible cytokine gene regulation (Figure 6C). In contrast, the expression of histidine decarboxylase (*Hdc*), which is the rate-limiting enzyme for histamine biosynthesis, was scarcely affected by MTX treatment compared with other cytokines, indicating that MTX does not globally reduce the transcript levels in mast cells (Figure 6C). These results suggest that GATA2 promotes cytokine induction in response to LPS stimulation in multiple types of mast cells.

## The -39 kb region of the *Il6* locus is essential for basal and induced *Il6* expression in BRC6 cells

To delineate the role played by the cluster of GATA2- and PU.1-binding peaks at the -39 kb region of the *Il6* locus, we deleted the -39 kb region encompassing 510 bp nucleotide sequences using the CRISPR/Cas-9-based excision system in BRC6 cells (Figures 7A and 7E). We obtained ten clones with homozygous -39 kb deletions, which were confirmed using PCR and Sanger sequencing (Figure S3A). Eight out of the ten homozygous clones were mixed and subjected to subsequent analysis (del/del, hereafter) (Figure S3A). LPS treatment (1 μg/mL) significantly induced the mRNA expression of *Il6*, *Il13*, and *Tnf* at 2 h, which returned to basal levels at 7 h in WT BRC6 cells (Figure 7C). Notably, LPS-induced *Il6* mRNA expression was significantly reduced in the del/del mutant cells at 2 and 7 h, but the expression of other cytokines, including *Il13* and *Tnf*, was unaffected (Figure 7C). These results indicated that the -39 kb element played an essential role in *Il6* mRNA expression in BRC6 mast cells. *GATA2* and *PU.1* mRNA expression levels were slightly increased at 2 h after LPS treatment, and this expression was not affected in the del/del mutant (Figure 7B).

### Deletion of -39 kb modestly decreases *Il6* expression in macrophages

Macrophages are a major source of IL-6 at inflammatory sites, but GATA2 is rarely expressed in peritoneal macrophages (Takai et al., 2021). To address differences in cytokine gene regulation in mast cells and macrophages, we examined the induced expression profile of *Il6*, *Tnf*, and *Il1b* after LPS treatment in the RAW264.7 murine macrophage cell line. The mRNA expression of *Il6*, *Tnf*, and *Il1b* was induced 2 h after LPS treatment (500 ng/mL). *Il6* and *Il1b* expression levels were further increased at 7 h (Figure 7D). These results indicated that RAW264.7 cells exhibited a relatively slow and prolonged response to LPS compared with BRC6 cells (compare Figures 7C and 7D). We next examined whether the -39 kb region exerted any regulatory activity in RAW264.7 macrophages. We deleted the -39 kb element in RAW264.7 cells using the CRISPR/Cas-9 system and stimulated the cells with LPS (Figures 7D and S3B). The LPS-stimulated *Il6* expression was decreased to 50% in the del/+ and del/del RAW264.7 cells, which indicated that the -39 kb element played a positive regulatory role in *Il6* induction in RAW264.7 cells, but the overall effects were modest compared with those in BRC6 cells (Figure 7D). *Tnf* and *Il1b* levels were slightly increased in the del/del RAW264.7 cells, which was likely potential compensation for the reduced IL6 levels. These results indicated that the -39 kb element played a regulatory role in RAW264.7 macrophages, which was modest compared with BRC6 mast cells.

### The -39 kb region of *Il6* is essential for the maintenance of open chromatin structure in BRC6 cells

We next investigated whether the -39 kb region regulated the chromatin configuration in the *Il6* locus. To this end, we performed chromatin immunoprecipitation analyses using an anti-panacetylated histone H3 antibody. The -39 kb, -19 kb, promoter, and first intron regions of the *Il6* locus showed an accumulation of acetylated H3 irrespective of LPS treatment in wild-type BRC6 cells (Figure 8A left). This result indicates that the chromatin structure in the *Il6* locus is already permissive for transcription before LPS stimulation. In contrast, acetylated H3 binding in the -39 kb del/del cells was significantly reduced in the *Il6* locus encompassing 5′ 39 kb to the first intron region (Figure 8A right). This result indicates that the -39 kb region is responsible for the open chromatin configuration of a broad region of the *Il6* locus.

## DISCUSSION

GATA2 plays an essential role in the differentiation and maintenance of mast cells, but the mechanisms underlying GATA2-mediated regulation of its target genes under inflammatory and infectious stimuli has been less explored. The present study addressed this question by conducting GATA2 and PU.1 ChIP-seq analysis in a murine mast cell line after treatment with the mycobacterial product LPS. We identified a class of enhancers that enriched GATA2- and PU.1-binding peaks in the relatively distal flanking regions of inflammation-associated genes. This class of enhancers was associated with increased chromatin accessibility with H3K27ac modification regardless of LPS stimulation. Among these enhancers, we found a novel *cis*-regulatory element at the 39 kb 5′ region of the *Il6* gene that contained clustered GATA2- and PU.1-binding sites and exhibited essential requirements for basal- and LPS-induced *Il6* expression in BRC6 mast cells. Our data revealed the vital function of the *Il6* -39 kb region in maintaining the active chromatin architecture at the *Il6* locus in mast cells.

Mast cells participate in the immune defense against bacterial infection, in addition to their known role in allergies and asthma. For example, mast-cell-derived TNF-α-dependent recruitment of leukocytes with bactericidal activity is crucial for defense against infection (Echtenacher et al., 1996; Malaviya et al., 1996). Mast cells exert the innate immune response via various pattern recognition receptors, including Toll-like receptors (TLRs). Numerous studies have shown that TLR4 stimulation by LPS activates NF-κB signaling in human and murine mast cells, whereas TLR ligands marginally induce the activity of the activator protein 1 (AP-1) transcription factor in mast cells (Supajatura et al., 2001; Qiao et al., 2006; Sandig and Bulfone-Paus, 2012). Functional *cis*-regulatory elements for these signal-responsive transcription factors were identified in the immediate upstream region of the human and mouse *Il6* promoters (Luo and Zheng., 2016). Deletion of the -39 kb element containing the clustered GATA2- and PU.1-binding sites resulted in a closed chromatin structure of the *Il6* locus, including the promoter regions in the mast cells. Given these data, we suggest that GATA2 and PU.1 bound to the -39 kb element promote permissive chromatin configuration in the broad range of *Il6* loci and facilitate recruitment of the signal-responsive transcription factors to the promoter region (Figure 8B). Consistent with our hypothesis, various
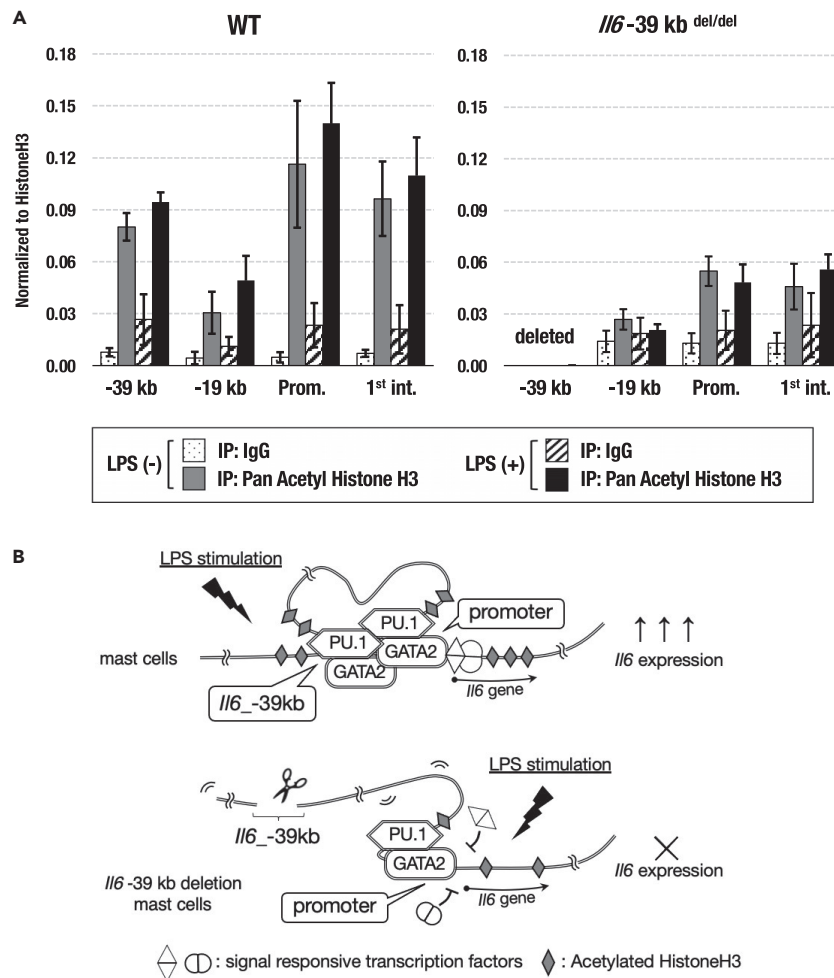
**Figure 8. The -39 kb region is essential for the open chromatin configuration of the *Il6* locus**

(A) The -39 kb, -19 kb, promoter, and first intron regions of the *Il6* locus showed accumulation of acetylated histone H3 irrespective of LPS treatment in the wild-type BRC6 cells (left) by ChIP–qPCR analysis. In contrast, the acetylated H3 binding was significantly diminished in the *Il6* locus in the -39 kb del/del cells (right).

(B) (upper) GATA2 and PU.1 bound to the -39 kb element promote permissive chromatin configuration in the broad range of the *Il6* locus, including the promoter region. Signal-responsive transcription factors (e.g., NF-κB and AP-1) bind to the primed *Il6* locus and induce robust *Il6* expression. (lower) Deletion of the -39 kb element diminishes GATA2 and PU.1 binding, thereby reducing the histone lysine acetylation. Consequently, signal-responsive transcription factors fail to induce *Il6* expression.

signal-responsive transcription factors, e.g., SMADs, TCFs, and NF-κB, interact preferentially with the genomic regions that are already primed by the prior binding of other lineage-determining transcription factors (Choudhuri et al., 2020; Alizada et al., 2021).

Deletion of the -39 kb region reduced *Il6* expression predominantly in mast cells, and the effect was less significant in the macrophage cell line, which indicates that the -39 kb regulatory region acts preferentially in mast cells. The -39 kb region harbors two ETS-binding sites and five GATA-binding sites. Our ChIP data showed that GATA2 and PU.1 robustly bound to the -39 kb region, which suggests that the regulatory activity of the -39 kb region relies on GATA2 and PU.1. PU.1 is abundantly expressed in macrophages, whereas GATA2 levels are much lower in macrophages than in mast cells (Takai et al., 2021). GATA2-deficient yolk sac progenitors still give rise to macrophages, which supports that GATA2 is dispensable for macrophage development (Kaimakis et al., 2016). The lack of a sufficient level of GATA2 may eliminate the regulatory activity of the -39 kb region in macrophages.

How the -39 kb region organizes the chromosomal configuration of the broad *Il6* locus remains obscure. PU.1 recruits the chromatin looping factor LDB1 to the *Spi1* locus, which confers an active chromatin configuration and facilitates autoregulation (Schuetzmann et al., 2018). We also reported that PU.1 bound to the *Ms4a2* gene locus recruits LDB1, which promotes GATA binding and robust *Ms4a2* expression (Ohmori et al., 2019). Therefore, a similar mechanism may operate in the *Il6* locus. Meanwhile, CCCTC-binding factor (CTCF) often organizes chromosomal architecture in numerous contexts (Zhu and Wang, 2019). We recently demonstrated that CTCF binding to a distal regulatory region of the *Tpsb2* locus, which encodes a mast cell tryptase, was facilitated by prior GATA1 binding in the vicinity region (Ohneda et al., 2019). Whether GATA2 and PU.1 confer a permissive chromatin configuration in the *Il6* locus via CTCF is an intriguing question.

GATA transcription factors function as pioneer factors and access their target sites in the context of nucleosomes, but other factors require more accessible DNA for binding (Tanaka et al., 2020). Once bound, pioneer transcription factors promote chromatin accessibility and accelerate subsequent gene transcription. Our observation that GATA2 was bound to the enhancers in unstimulated BRC6 mast cells suggests its role as a pioneer factor promoting access of other signal-responsive transcription factors in mast cells. The present study showed that GATA2 knockdown diminished LPS-induced cytokine gene induction in BRC6 cells. The Cre-loxP-mediated deletion of GATA2 or PU.1 decreased LPS-induced cytokine expression in peritoneal mast cells. GATA2 and PU.1 double deletion further suppressed LPS-induced *Il6* induction. Notably, peritoneal mast cells represent more mature and physiological conditions of tissue mast cells (Sandig and Bulfone-Paus, 2012). Therefore, these results suggest that GATA2 and PU.1 collaboratively enhance LPS-induced *Il6* expression in tissue mast cells. We also found that the binding pattern and affinity of GATA2 and PU.1 to chromatin were not significantly different irrespective of LPS treatment. These results indicate that GATA2 and PU.1 create an accessible chromatin state at the inflammatory cytokine gene loci and augment the immediate responses to LPS-induced inflammatory stimuli in mast cells.

A large-scale genome-wide association study (GWAS) of C-reactive protein (CRP) levels identified a significant association between serum CRP levels and single-nucleotide polymorphisms (SNPs) in the 5' regulatory region of the human *IL6* locus (rs2097677) (Okada et al., 2010). Closer observation showed that the most significantly associated SNPs resided approximately 30 kb 5' to the human *IL6* gene. We found that the 3' end nucleotide sequences in the mouse -39 kb region were partially conserved in the human *IL6* locus -30 kb region, whereas the mouse ortholog of human rs2097677 was not clearly identified (Figure 7E). The human *IL6* promoter polymorphism (174G>C; rs1800795) is associated with numerous inflammatory and autoimmune diseases (Tanaka et al., 2014). Additional functional regulatory polymorphisms that affect IL-6 levels may also exist in distal flanking regions. The mouse -39 kb orthologous region in the human *IL6* locus, possibly approximately the 5' 30 kb, would be a plausible candidate region that harbors disease-related rSNPs.

Our findings collectively reveal the partial mechanism underlying how GATA2 contributes to the high levels of *Il6* gene transcription and its robust responsiveness to microbial stimulation in mast cells. Due to the diverse pathophysiological activities of IL-6 in multiple tissue contexts, how mast-cell-derived IL-6 contributes to host defense and accelerates systemic or local inflammation should be carefully investigated. Given that IL-6 aberrations underlie inflammation, the pharmacological inhibition of GATA2, as we demonstrated here, might offer therapeutic protection against various inflammatory diseases.

More detailed studies on the *Il6* -39 kb region in the mouse model will provide a deeper understanding of the innate immune system dictated by IL-6 produced from mast cells and may open new therapeutic avenues for infectious and inflammatory diseases.

### Limitations of the study

This study demonstrated that GATA2-PU.1 overlapping binding sites tended to be located in the distal *cis*-regulatory regions of inflammatory cytokine gene loci in murine mast cells. In particular, the GATA2-PU.1-clustered binding sites at the 5' 39 kb region of the *Il6* locus play a central role in LPS-induced *Il6* expression in the mast cells. However, because these results have been demonstrated in the primary mouse mast cells and mast cell lines, further studies will be needed to clarify whether the *Il6* 5' 39 kb region confers mast-cell-specific regulatory activity in an *in vivo* animal model. In addition, deeper molecular insights underlying the mast-cell-specific regulatory activities of the *Il6* 5' 39 kb region should be clarified.

## STAR★METHODS

Detailed methods are provided in the online version of this paper and include the following:

- KEY RESOURCES TABLE
- RESOURCE AVAILABILITY
  - Lead contact
  - Materials availability
  - Data and code and availability
- EXPERIMENTAL MODEL AND SUBJECT DETAILS
  - Mice
  - Cell lines
- METHOD DETAILS
  - Peritoneal cell-derived mast cell
  - RNA extraction and quantitative real-time RT–PCR (RT–qPCR)
  - Transfection of siRNAs
  - Chromatin immunoprecipitation (ChIP) assay
  - Chromatin immunoprecipitation sequencing
  - Bioinformatics analysis
  - Preparation of CRISPR–Cas9 ribonucleoprotein (RNP)
- QUANTIFICATION AND STATISTICAL ANALYSIS

## SUPPLEMENTAL INFORMATION

Supplemental information can be found online at https://doi.org/10.1016/j.isci.2022.104942.

## AUTHOR CONTRIBUTIONS

S.O., J.T., and S.U. conducted the experiments. A.O. collected the NGS raw data. A.O. and T.M. performed bioinformatics analysis. S.O., J.T., S.O., T.M., K.O., and T.M. contributed to the project design. T.M. wrote the draft and finalized the manuscript. All authors contributed to the integration and discussion of the results.

## DECLARATION OF INTERESTS

The authors declare no conflicts of interest associated with this manuscript.

## REFERENCES

Abraham, S.N., and St John, A.L. (2010). Mast cell-orchestrated immunity to pathogens. Nat. Rev. Immunol. *10*, 440–452. https://doi.org/10.1038/nri2782.

Alizada, A., Khyzha, N., Wang, L., Antounians, L., Chen, X., Khor, M., Liang, M., Rathnakumar, K., Weirauch, M.T., Medina-Rivera, A., et al. (2021). Conserved regulatory logic at accessible and inaccessible chromatin during the acute inflammatory response in mammals. Nat.

Commun. *12*, 567. https://doi.org/10.1038/s41467-020-20765-1.

Arinobu, Y., Mizuno, S.i., Chong, Y., Shigematsu, H., Iino, T., Iwasaki, H., Graf, T., Mayfield, R., Chan, S., Kastner, P., et al. (2007). Reciprocal activation of GATA-1 and PU.1 marks initial specification of hematopoietic stem cells into myeloerythroid and myelolymphoid lineages. Cell Stem Cell *1*, 416–427. https://doi.org/10.1016/j.stem.2007.07.004.

Baba, Y., Maeda, K., Yashiro, T., Inage, E., Niyonsaba, F., Hara, M., Suzuki, R., Ohtsuka, Y., Shimizu, T., Ogawa, H., et al. (2012). Involvement of PU.1 in mast cell/basophil-specific function of the human IL1RL1/ST2 promoter. Allergol. Int. *61*, 461–467. https://doi.org/10.2332/allergolint.12-OA-0424.

Barton, G.M., and Medzhitov, R. (2003). Toll-like receptor signaling pathways. Science *300*, 1524–1525. https://doi.org/10.1126/science.1085536.

Bischoff, S.C. (2007). Role of mast cells in allergic and non-allergic immune responses: comparison of human and murine data. Nat. Rev. Immunol. 7, 93–104. https://doi.org/10.1038/nri2018.

Burda, P., Vargova, J., Curik, N., Salek, C., Papadopoulos, G.L., Strouboulis, J., and Stopka, T. (2016). GATA-1 inhibits PU.1 gene via DNA and histone H3K9 methylation of its distal enhancer in erythroleukemia. PLoS One 11, e0152234. https://doi.org/10.1371/journal.pone.0152234.

Cardamone, C., Parente, R., Feo, G.D., and Triggiani, M. (2016). Mast cells as effector cells of innate immunity and regulators of adaptive immunity. Immunol. Lett. 178, 10–14. https://doi.org/10.1016/j.imlet.2016.07.003.

Charles, M.A., Saunders, T.L., Wood, W.M., Owens, K., Parlow, A.F., Camper, S.A., Ridgway, E.C., and Gordon, D.F. (2006). Pituitary-specific Gata2 knockout: effects on gonadotrope and thyrotrope function. Mol. Endocrinol. 20, 1366–1377. https://doi.org/10.1210/me.2005-0378.

Castro-Mondragon, J.A., Riudavets-Puig, R., Rauluseviciute, I., Lemma, R.B., Turchi, L., Blanc-Mathieu, R., Lucas, J., Boddie, P., Khan, A., Manosalva Pérez, N., et al. (2022). JASPAR 2022: the 9th release of the open-access database of transcription factor binding profiles. Nucleic Acids Res. 50, D165–D173. https://doi.org/10.1093/nar/gkab1113.

Choudhuri, A., Trompouki, E., Abraham, B.J., Colli, L.M., Kock, K.H., Mallard, W., Yang, M.L., Vinjamur, D.S., Ghamari, A., Sporrij, A., et al. (2020). Common variants in signaling transcription-factor-binding sites drive phenotypic variability in red blood cell traits. Nat. Genet. 52, 1333–1345. https://doi.org/10.1038/s41588-020-00738-2.

Dienz, O., Rud, J.G., Eaton, S.M., Lanthier, P.A., Burg, E., Drew, A., Bunn, J., Suratt, B.T., Haynes, L., and Rincon, M. (2012). Essential role of IL-6 in protection against H1N1 influenza virus by promoting neutrophil survival in the lung. Mucosal Immunol. 5, 258–266. https://doi.org/10.1038/mi.2012.2.

Doré, L.C., and Crispino, J.D. (2011). Transcription factor networks in erythroid cell and megakaryocyte development. Blood 118, 231–239. https://doi.org/10.1182/blood-2011-04-285981.

Duttke, S.H., Chang, M.W., Heinz, S., and Benner, C. (2019). Identification and dynamic quantification of regulatory elements using total RNA. Genome Res. 29, 1836–1846. https://doi.org/10.1101/gr.253492.119.

Echtenacher, B., Männel, D.N., and Hültner, L. (1996). Critical protective role of mast cells in a model of acute septic peritonitis. Nature 381, 75–77. https://doi.org/10.1038/381075a0.

Glass, C.K., and Saijo, K. (2010). Nuclear receptor transrepression pathways that regulate inflammation in macrophages and T cells. Nat. Rev. Immunol. 10, 365–376. https://doi.org/10.1038/nri2748.

Hameyer, D., Loonstra, A., Eshkind, L., Schmitt, S., Antunes, L., Groen, A., Bindels, E., Jonkers, J., Krimpenfort, P., Meuwissen, R., et al. (2007). Toxicity of ligand-dependent Cre recombinases and generation of a conditional Cre deleter mouse allowing mosaic recombination in peripheral tissues. Physiol. Genomics 31, 32–41. https://doi.org/10.1152/physiolgenomics.00019.2007.

Hayashi, M., Takai, J., Yu, L., Motohashi, H., Moriguchi, T., and Yamamoto, M. (2015). Whole-body in vivo monitoring of inflammatory diseases exploiting human interleukin 6-luciferase transgenic mice. Mol. Cell Biol. 35, 3590–3601. https://doi.org/10.1128/MCB.00506-15.

Heinz, S., Benner, C., Spann, N., Bertolino, E., Lin, Y.C., Laslo, P., Cheng, J.X., Murre, C., Singh, H., and Glass, C.K. (2010). Simple combinations of lineage-determining transcription factors prime cis-regulatory elements required for macrophage and B cell identities. Mol. Cell 38, 576–589. https://doi.org/10.1016/j.molcel.2010.05.004.

Hirano, T., Taga, T., Nakano, N., Yasukawa, K., Kashiwamura, S., Shimizu, K., Nakajima, K., Pyun, K.H., and Kishimoto, T. (1985). Purification to homogeneity and characterization of human B-cell differentiation factor (BCDF or BSFp-2). Proc. Natl. Acad. Sci. USA 82, 5490–5494. https://doi.org/10.1073/pnas.82.16.5490.

Hiroyama, T., Miharada, K., Sudo, K., Danjo, I., Aoki, N., and Nakamura, Y. (2008). Establishment of mouse embryonic stem cell-derived erythroid progenitor cell lines able to produce functional red blood cells. PLoS One 3, e1544. https://doi.org/10.1371/journal.pone.0001544.

Iwasaki, H., Somoza, C., Shigematsu, H., Duprez, E.A., Iwasaki-Arai, J., Mizuno, S.I., Arinobu, Y., Geary, K., Zhang, P., Dayaram, T., et al. (2005). Distinctive and indispensable roles of PU.1 in maintenance of hematopoietic stem cells and their differentiation. Blood 106, 1590–1600. https://doi.org/10.1182/blood-2005-03-0860.

Kaimakis, P., de Pater, E., Eich, C., Solaimani Kartalaei, P., Kauts, M.L., Vink, C.S., van der Linden, R., Jaegle, M., Yokomizo, T., Meijer, D., et al. (2016). Functional and molecular characterization of mouse Gata2-independent hematopoietic progenitors. Blood 127, 1426–1437. https://doi.org/10.1182/blood-2015-10-673749.

Kaneko, H., Katoh, T., Hirano, I., Hasegawa, A., Tsujita, T., Yamamoto, M., and Shimizu, R. (2017). Induction of erythropoietin gene expression in epithelial cells by chemicals identified in GATA inhibitor screenings. Gene Cell. 22, 939–952. https://doi.org/10.1111/gtc.12537.

Kishimoto, T. (2010). IL-6: from its discovery to clinical applications. Int. Immunol. 22, 347–352. https://doi.org/10.1093/intimm/dxq030.

Kopf, M., Baumann, H., Freer, G., Freudenberg, M., Lamers, M., Kishimoto, T., Zinkernagel, R., Bluethmann, H., and Köhler, G. (1994). Impaired immune and acute-phase responses in interleukin-6-deficient mice. Nature 368, 339–342. https://doi.org/10.1038/368339a0.

Krystel-Whittemore, M., Dileepan, K.N., and Wood, J.G. (2016). Mast cell: a multi-functional master cell. Front. Immunol. 6, 620. https://doi.org/10.3389/fimmu.2015.00620.

Langmead, B., and Salzberg, S.L. (2012). Fast gapped-read alignment with Bowtie 2. Nat. Methods 9, 357–359. https://doi.org/10.1038/nmeth.1923.

Ladel, C.H., Blum, C., Dreher, A., Reifenberg, K., Kopf, M., and Kaufmann, S.H. (1997). Lethal tuberculosis in interleukin-6-deficient mutant mice. Infect. Immun. 65, 4843–4849. https://doi.org/10.1128/iai.65.11.4843-4849.1997.

Li, Y., Qi, X., Liu, B., and Huang, H. (2015). The STAT5-GATA2 pathway is critical in basophil and mast cell differentiation and maintenance. J. Immunol. 194, 4328–4338. https://doi.org/10.4049/jimmunol.1500018.

Lunderius, C., Xiang, Z., Nilsson, G., and Hellman, L. (2000). Murine mast cell lines as indicators of early events in mast cell and basophil development. Eur. J. Immunol. 30, 3396–3402. https://doi.org/10.1002/1521-4141(2000012)30:12<3396::AID-IMMU3396>3.0.CO;2-O.

Luo, Y., and Zheng, S.G. (2016). Hall of fame among pro-inflammatory cytokines: interleukin-6 gene and its transcriptional regulation mechanisms. Front. Immunol. 7, 604. https://doi.org/10.3389/fimmu.2016.00604.

Malaviya, R., Ikeda, T., Ross, E., and Abraham, S.N. (1996). Mast cell modulation of neutrophil influx and bacterial clearance at sites of infection through TNF-alpha. Nature 381, 77–80. https://doi.org/10.1038/381077a0.

Malbec, O., Roget, K., Schiffer, C., Iannascoli, B., Dumas, A.R., Arock, M., and Daëron, M. (2007). Peritoneal cell-derived mast cells: an in vitro model of mature serosal-type mouse mast cells. J. Immunol. 178, 6465–6475. https://doi.org/10.4049/jimmunol.178.

McLean, C.Y., Bristor, D., Hiller, M., Clarke, S.L., Schaar, B.T., Lowe, C.B., Wenger, A.M., and Bejerano, G. (2010). GREAT improves functional interpretation of cis-regulatory regions. Nat. Biotechnol. 28, 495–501. https://doi.org/10.1038/nbt.1630.

Medzhitov, R., and Horng, T. (2009). Transcriptional control of the inflammatory response. Nat. Rev. Immunol. 9, 692–703. https://doi.org/10.1038/nri2634.

Minegishi, N., Suzuki, N., Kawatani, Y., Shimizu, R., and Yamamoto, M. (2005). Rapid turnover of GATA-2 via ubiquitin-proteasome protein degradation pathway. Gene Cell. 10, 693–704. https://doi.org/10.1111/j.1365-2443.2005.00864.x.

Mukai, K., Tsai, M., Starkl, P., Marichal, T., and Galli, S.J. (2016). IgE and mast cells in host defense against parasites and venoms. Semin. Immunopathol. 38, 581–603. https://doi.org/10.1007/s00281-016-0565-1.

Nerlov, C., Querfurth, E., Kulessa, H., and Graf, T. (2000). GATA-1 interacts with the myeloid PU.1 transcription factor and represses PU.1-dependent transcription. Blood 95, 2543–2551. https://doi.org/10.1182/blood.V95.8.2543.

Ohmori, S., Takai, J., Ishijima, Y., Suzuki, M., Moriguchi, T., Philipsen, S., Yamamoto, M., and Ohneda, K. (2012). Regulation of GATA factor expression is distinct between erythroid and mast cell lineages. Mol. Cell Biol. 32, 4742–4755. https://doi.org/10.1128/MCB.00718-12.

Ohmori, S., Ishijima, Y., Numata, S., Takahashi, M., Sekita, M., Sato, T., Chugun, K., Yamamoto, M., and Ohneda, K. (2019). GATA2 and PU.1

collaborate to activate the expression of the mouse *Ms4a2*Gene, encoding FcεRIβ, through distinct mechanisms. Mol. Cell Biol. *39*, e00314–e00319. https://doi.org/10.1128/MCB.00314-19.

Ohmori, S., Moriguchi, T., Noguchi, Y., Ikeda, M., Kobayashi, K., Tomaru, N., Ishijima, Y., Ohneda, O., Yamamoto, M., and Ohneda, K. (2015). GATA2 is critical for the maintenance of cellular identity in differentiated mast cells derived from mouse bone marrow. Blood *125*, 3306–3315. https://doi.org/10.1182/blood-2014-11-612465.

Ohneda, K., Ohmori, S., and Yamamoto, M. (2019). Mouse tryptase gene expression is coordinately regulated by GATA1 and GATA2 in bone marrow-derived mast cells. Int. J. Mol. Sci. *20*, 4603. https://doi.org/10.3390/ijms20184603.

Okada, Y., Takahashi, A., Ohmiya, H., Kumasaka, N., Kamatani, Y., Hosono, N., Tsunoda, T., Matsuda, K., Tanaka, T., Kubo, M., et al. (2010). Genome-wide association study for C-reactive protein levels identified pleiotropic associations in the IL6 locus. Hum. Mol. Genet. *20*, 1224–1231. https://doi.org/10.1093/hmg/ddq551.

Otsuki, A., Suzuki, M., Katsuoka, F., Tsuchida, K., Suda, H., Morita, M., Shimizu, R., and Yamamoto, M. (2016). Unique cistrome defined as CsMBE is strictly required for Nrf2-sMaf heterodimer function in cytoprotection. Free Radic. Biol. Med. *91*, 45–57. https://doi.org/10.1016/j.freeradbiomed.2015.12.005.

Qiao, H., Andrade, M.V., Lisboa, F.A., Morgan, K., and Beaven, M.A. (2006). FcepsilonR1 and toll-like receptors mediate synergistic signals to markedly augment production of inflammatory cytokines in murine mast cells. Blood *107*, 610–618. https://doi.org/10.1182/blood-2005-06-2271.

Rada-Iglesias, A., Bajpai, R., Swigut, T., Brugmann, S.A., Flynn, R.A., and Wysocka, J. (2011). A unique chromatin signature uncovers early developmental enhancers in humans. Nature *470*, 279–283. https://doi.org/10.1038/nature09692.

Rekhtman, N., Radparvar, F., Evans, T., and Skoultchi, A.I. (1999). Direct interaction of hematopoietic transcription factors PU.1 and GATA-1: functional antagonism in erythroid cells. Genes Dev. *13*, 1398–1411. https://doi.org/10.1101/gad.13.11.1398.

Rodewald, H.R., and Feyerabend, T.B. (2012). Widespread immunological functions of mast cells: fact or fiction? Immunity *37*, 13–24. https://doi.org/10.1016/j.immuni.2012.07.007.

Rose-John, S., Winthrop, K., and Calabrese, L. (2017). The role of IL-6 in host defence against infections: immunobiology and clinical implications. Nat. Rev. Rheumatol. *13*, 399–409. https://doi.org/10.1038/nrrheum.2017.83.

Samuel, J.M., Kelberman, D., Smith, A.J.P., Humphries, S.E., and Woo, P. (2008). Identification of a novel regulatory region in the interleukin-6 gene promoter. Cytokine *42*,

256–264. https://doi.org/10.1016/j.cyto.2008.02.008.

Sandig, H., and Bulfone-Paus, S. (2012). TLR signaling in mast cells: common and unique features. Front. Immunol. *3*, 185. https://doi.org/10.3389/fimmu.2012.00185.

Schuetzmann, D., Walter, C., van Riel, B., Kruse, S., König, T., Erdmann, T., Tönges, A., Bindels, E., Weilemann, A., Gebhard, C., et al. (2018). Temporal autoregulation during human PU.1 locus SubTAD formation. Blood *132*, 2643–2655. https://doi.org/10.1182/blood-2018-02-834721.

Shibagaki, S., Tahara-Hanaoka, S., Hiroyama, T., Nakamura, Y., and Shibuya, A. (2017). Long-term survival of the mouse ES cell-derived mast cell, MEDMC-BRC6, in mast cell-deficient KitW-sh/W-sh mice. Int. Immunol. *29*, 235–242. https://doi.org/10.1093/intimm/dxx022.

Smale, S.T. (2010). Selective transcription in response to an inflammatory stimulus. Cell *140*, 833–844. https://doi.org/10.1016/j.cell.2010.01.037.

Supajatura, V., Ushio, H., Nakao, A., Okumura, K., Ra, C., and Ogawa, H. (2001). Protective roles of mast cells against enterobacterial infection are mediated by Toll-like receptor 4. J. Immunol. *167*, 2250–2256. https://doi.org/10.4049/jimmunol.167.4.2250.

Takai, J., Moriguchi, T., Suzuki, M., Yu, L., Ohneda, K., and Yamamoto, M. (2013). The Gata1 5′ region harbors distinct cis-regulatory modules that direct gene activation in erythroid cells and gene inactivation in HSCs. Blood *122*, 3450–3460. https://doi.org/10.1182/blood-2013-01-476911.

Takai, J., Ohtsu, H., Sato, A., Uemura, S., Fujimura, T., Yamamoto, M., and Moriguchi, T. (2019). Lipopolysaccharide-induced expansion of histidine decarboxylase-expressing Ly6G+myeloid cells identified by exploiting histidine decarboxylase BAC-GFP transgenic mice. Sci. Rep. *9*, 15603. https://doi.org/10.1038/s41598-019-51716-6.

Takai, J., Shimada, T., Nakamura, T., Engel, J.D., and Moriguchi, T. (2021). *Gata2* heterozygous mutant mice exhibit reduced inflammatory responses and impaired bacterial clearance. iScience *24*, 102836. https://doi.org/10.1016/j.isci.2021.102836.

Tanaka, T., Narazaki, M., and Kishimoto, T. (2014). IL-6 in inflammation, immunity, and disease. Cold Spring Harb. Perspect. Biol. *6*, a016295. https://doi.org/10.1101/cshperspect.a016295.

Tanaka, H., Takizawa, Y., Takaku, M., Kato, D., Kumagawa, Y., Grimm, S.A., Wade, P.A., and Kurumizaka, H. (2020). Interaction of the pioneer transcription factor GATA3 with nucleosomes. Nat. Commun. *11*, 4136. https://doi.org/10.1038/s41467-020-17959-y.

Thorvaldsdóttir, H., Robinson, J.T., and Mesirov, J.P. (2013). Integrative Genomics Viewer (IGV): high-performance genomics data visualization

and exploration. Brief. Bioinform. *14*, 178–192. https://doi.org/10.1093/bib/bbs017.

Walsh, J.C., DeKoter, R.P., Lee, H.J., Smith, E.D., Lancki, D.W., Gurish, M.F., Friend, D.S., Stevens, R.L., Anastasi, J., and Singh, H. (2002). Cooperative and antagonistic interplay between PU.1 and GATA-2 in the specification of myeloid cell fates. Immunity *17*, 665–676. https://doi.org/10.1016/S1074-7613(02)00452-1.

Wu, W., Morrissey, C.S., Keller, C.A., Mishra, T., Pimkin, M., Blobel, G.A., Weiss, M.J., and Hardison, R.C. (2014). Dynamic shifts in occupancy by TAL1 are guided by GATA factors and drive large-scale reprogramming of gene expression during hematopoiesis. Genome Res. *24*, 1945–1962. https://doi.org/10.1101/gr.164830.113.

Yu, L., Moriguchi, T., Kaneko, H., Hayashi, M., Hasegawa, A., Nezu, M., Saya, H., Yamamoto, M., and Shimizu, R. (2017). Reducing inflammatory cytokine production from renal collecting duct cells by inhibiting GATA2 ameliorates acute kidney injury. Mol. Cell Biol. *37*, e00211–e00217. https://doi.org/10.1128/MCB.00211-17.

Zhang, P., Behre, G., Pan, J., Iwama, A., Wara-Aswapati, N., Radomska, H.S., Auron, P.E., Tenen, D.G., and Sun, Z. (1999). Negative cross-talk between hematopoietic regulators: GATA proteins repress PU.1. Proc. Natl. Acad. Sci. USA *96*, 8705–8710. https://doi.org/10.1073/pnas.96.15.8705.

Zhang, P., Zhang, X., Iwama, A., Yu, C., Smith, K.A., Mueller, B.U., Narravula, S., Torbett, B.E., Orkin, S.H., and Tenen, D.G. (2000). PU.1 inhibits GATA-1 function and erythroid differentiation by blocking GATA-1 DNA binding. Blood *96*, 2641–2648. https://doi.org/10.1182/blood.V96.8.2641.

Zhang, Y., Liu, T., Meyer, C.A., Eeckhoute, J., Johnson, D.S., Bernstein, B.E., Nusbaum, C., Myers, R.M., Brown, M., Li, W., et al. (2008). Model-based analysis of ChIP-seq (MACS). Genome Biol. *9*, R137. https://doi.org/10.1186/gb-2008-9-9-r137.

Zhu, Z., and Wang, X. (2019). Roles of cohesin in chromosome architecture and gene expression. Semin. Cell Dev. Biol. *90*, 187–193. https://doi.org/10.1016/j.semcdb.2018.08.004.

Zimmermann, C., Troeltzsch, D., Giménez-Rivera, V.A., Galli, S.J., Metz, M., Maurer, M., and Siebenhaar, F. (2019). Mast cells are critical for controlling the bacterial burden and the healing of infected wounds. Proc. Natl. Acad. Sci. USA *116*, 20500–20504. https://doi.org/10.1073/pnas.1908816116.

Zon, L.I., Gurish, M.F., Stevens, R.L., Mather, C., Reynolds, D.S., Austen, K.F., and Orkin, S.H. (1991). GATA-binding transcription factors in mast cells regulate the promoter of the mast cell carboxypeptidase A gene. J. Biol. Chem. *266*, 22948–22953. https://doi.org/10.1016/S0021-9258(18)54446-X.

## STAR★METHODS

### KEY RESOURCES TABLE

| REAGENT or RESOURCE | SOURCE | IDENTIFIER |
|---|---|---|
| **Antibodies** | | |
| Mouse monoclonal anti-GATA2 | Perseus Proteomics | Cat#PP-B9922A-0C; RRID: N/A |
| Mouse monoclonal anti-PU.1 (clone C-3) | Santa Cruz Biotechnology | Cat#sc-390405 X; RRID: N/A |
| Rabbit polyclonal anti-Histone H3 (acetyl K27) | Abcam | Cat# ab4729; RRID:AB_2118291 |
| Rabbit polyclonal anti-Histone H3 | Abcam | Cat# ab1791; RRID: AB_302613 |
| **Chemicals, peptides, and recombinant proteins** | | |
| 4-hydroxytamoxifen (4-OHT) | Sigma-Aldrich | Cat#H7904; CAS:68047-06-3 |
| interleukin-3 | Peprotech | Cat #213-13; GenPept: P01586 |
| SCF | Peprotech | Cat #250-03; GenPept: P20826 |
| Lipopolysaccharides, from *Escherichia coli* O55:B5 | Sigma-Aldrich | Cat#L2880; CAS:93572-42-0 |
| **Critical commercial assays** | | |
| NucleoSpin RNA Plus | MACHEREY-NAGEL | Cat#740984 |
| ReverTra Ace qPCR RT Master Mix | TOYOBO | Cat# FSQ-201 |
| THUNDERBIRD Next SYBR qPCR Mix | TOYOBO | Cat#QPX-201 |
| Dynabeads Protein A | Invitrogen | REF;10002D |
| Dynabeads M-280 Sheep anti-Mouse IgG | Invitrogen | REF;11201D |
| **Deposited data** | | |
| ChIP-seq raw data (MEDMC-BRC6 cells) | This paper | PRJDB12807 |
| **Experimental models: Cell lines** | | |
| MEDMC-BRC6 cells | RIKEN BioResource Center | RCB2694 |
| P815 cells | Tohoku Univ Cell Bank | TKG 0168 |
| Raw264.7 cells | ATCC | TIB-71 |
| MEL cells | ATCC | HB-132 |
| **Experimental models: Organisms/strains** | | |
| *Gata2* Floxed mice/C57BL/6J | Gift from S.A Camper | Charles et al., 2006 |
| *Spi1* Floxed mice/C57BL/6J | The Jackson Laboratory | JAX: 006922 |
| *Rosa26CreER*^T2^/C57BL/6J | Gift from Anton Berns | Hameyer et al., 2007 |
| **Oligonucleotides** | | |
| qChIP: *Il6* -39 kb Forward: GATTTGAAGCTGGTGGCATTC | This paper | N/A |
| qChIP: *Il6* -39 kb Reverse: CAGGATAGCAACACCCTCTTC | This paper | N/A |
| qChIP: *Il6* -19 kb Forward: AGGAGGCACTCTGGGAGTAC | This paper | N/A |
| qChIP: *Il6* -19 kb Reverse: TCAGTTCACCTTCCCCAGTTG | This paper | N/A |
| qChIP: *Il6* promoter Forward: AGGGCTAGCCTCAAGGATGAC | This paper | N/A |
| qChIP: *Il6* promoter Reverse: GTGGGGCTGATTGGAAACCT | This paper | N/A |
| qChIP: *Il6* 1st int Forward: CTCATTCTGCTCTGGAGCCC | This paper | N/A |
| qChIP: *Il6* 1st int Reverse: CTCAATAGCTCCGCCAGAGG | This paper | N/A |

*(Continued on next page)*

*Continued*

| REAGENT or RESOURCE | SOURCE | IDENTIFIER |
|---|---|---|
| qChIP: *Ms4a2* +10.4 kb Forward: CTTGGGCTGGTTTTATGTGTTC | This paper | N/A |
| qChIP: *Ms4a2* +10.4 kb Reverse: AGAACCAGGAGAGATAACATTGC | This paper | N/A |
| RT-qPCR: *Polr2a* Forward: CTGGACCCTCAAGCCCATACAT | This paper | N/A |
| RT-qPCR: *Polr2a* Reverse: CGTGGCTCATAGGCTGGTGAT | This paper | N/A |
| RT-qPCR: *Gata2* Forward: GCACCTGTTGTGCAAATTGT | This paper | N/A |
| RT-qPCR: *Gata2* Reverse: GCCCCTTTCTTGCTCTTCTT | This paper | N/A |
| RT-qPCR: *Spi1* Forward: AGAAGCTGATGGCTTGGAGC | This paper | N/A |
| RT-qPCR: *Spi1* Reverse: GCGAATCTTTTTCTTGCTGCC | This paper | N/A |
| RT-qPCR: *Il6* Forward: TACCACTTCACAAGTCGGAGGC | This paper | N/A |
| RT-qPCR: *Il6* Reverse: CTGCAAGTGCATCATCGTTGTTC | This paper | N/A |
| RT-qPCR: *Il13* Forward: CACTACGGTCTCCAGCCTCC | This paper | N/A |
| RT-qPCR: *Il13* Reverse: CTCATTAGAAGGGGCCGTGG | This paper | N/A |
| RT-qPCR: *Tnf* Forward: GGTGCCTATGTCTCAGCCTCTT | This paper | N/A |
| RT-qPCR: *Tnf* Reverse: GCCATAGAACTGATGAGAGGGAG | This paper | N/A |
| RT-qPCR: *Hdc* Forward: CGTTGCCTACACCTCTGATC | Takai et al., 2019 | N/A |
| RT-qPCR: *Hdc* Reverse: CCCTGTTGCTTGTCTTCCTC | Takai et al., 2019 | N/A |
| RT-qPCR: *Il1b* Forward: TGGACCTTCCAGGATGAGGACA | This paper | N/A |
| RT-qPCR: *Il1b* Reverse: GTTCATCTCGGAGCCTGTAGTG | This paper | N/A |
| siRNA targeting sequence: Gata2 #1: CCGGAAUCGGAAGAUGUCCAGCAAA | Life Technologies | Cat#GATA2MSS204584 |
| siRNA targeting sequence: Gata2 #2: GCCUCUACUACAAGCUGCACAAUGU | Life Technologies | Cat#GATA2MSS204585 |
| siRNA targeting sequence: PU.1 #1: CCUCCAUCGGAUGACUUGGUUACUU | Life Technologies | Cat#Sfpi1MSS247676 |
| siRNA targeting sequence: PU.1 #2: GCACACCAUGUCCACAACAACGAGU | Life Technologies | Cat#Sfpi1MSS247678 |
| siRNA targeting sequence: PU.1 #3: GGCGACAUGAAGGACAGCAUCUGGU | Life Technologies | Cat#Sfpi1MSS277025 |
| crRNA sequence targeting mouse *Il6* -39 kbp region (5'): AGATTATAACAAACGATGGT | IDT | N/A |
| crRNA sequence targeting mouse *Il6* -39 kbp region (3'): GTGGCTGGATTGGCAGAACT | IDT | N/A |
| Software and algorithms | | |
| GraphPad Prism 8 | GraphPad Software | N/A |
| KaleidaGraph Version 4.5 | HULINKS Inc. | N/A |
| Excel | Microsoft | N/A |
| Integrative Genomics Viewer (IGV) | Broad Institute | https://software.broadinstitute.org/software/igv/ |
| JASPAR | Castro-Mondragon et al., 2022 | https://jaspar.genereg.net |
| Python | Python Software Foundation | https://www.python.org/ |

**Continued**

| REAGENT or RESOURCE | SOURCE | IDENTIFIER |
|---|---|---|
| HOMER (Hypergeometric Optimization of Motif EnRichment) (v4.11) | Chris Benner, UCSD | http://homer.ucsd.edu/homer/motif/ |
| Pybedtools 0.9.0 | Ryan Dale, NIH | https://daler.github.io/pybedtools/ |
| GREAT version 4.0.4 | Gill Bejerano, Stanford University | http://great.stanford.edu/public/html/index.php |
| Other | | |
| Thermal Cycler Dice Real Time System III | TAKARA-BIO | Cat#TP950 |
| M220 Focused-ultrasonicator | Covaris | Part Number; 500295 |
| Alt-R trans-activating CRISPR RNA (tracrRNA) | IDT | Catalog #1072532 |
| Alt-R S.p. Cas9 Nuclease V3 | IDT | Catalog #1081058 |

## RESOURCE AVAILABILITY

### Lead contact

Further information and requests for resources and reagents should be directed to and will be fulfilled by the lead contact, Takashi Moriguchi (moriguchi@tohoku-mpu.ac.jp).

### Materials availability

This study did not generate new unique materials and reagents.

### Data and code and availability

- The ChIP-seq data generated in this publication have been deposited at DNA Data Base Japan (DDBJ) and are accessible as of the date of publication. Accession numbers are listed in the key resources table (PRJDB12807).

- This paper does not report original code.

- Any additional data generated or analyzed in this study are available upon request from the lead contact, Takashi Moriguchi (moriguchi@tohoku-mpu.ac.jp).

## EXPERIMENTAL MODEL AND SUBJECT DETAILS

### Mice

The 4-hydroxytamoxifen (4-OHT)-inducible $Rosa26CreER^{T2}$ mice were kindly provided by Anton Berns, Netherlands Cancer Institute (Hameyer et al., 2007). $Gata2^{flox/flox}$ mice (Charles et al., 2006) were kindly provided by S. A. Camper, University of Michigan. Spi1$^{flox/flox}$ mice (Iwasaki et al., 2005) were purchased from Jackson Laboratories (JAX: 006922). $Spi1^{flox/flox}$ mice harboring loxP sites surrounding $Spi1$ exons 4-5 were bred to $Rosa26$-$CreER^{T2}$ transgenic mice to obtain Spi1 $^{flox/flox}$::$CreER^{T2}$ mice. Littermate mice genotyped as $Gata2^{+/+}$::$CreER^{T2}$ or $Spi1^{+/+}$::$CreERT2$ mice were subjected to control peritoneal mast cell preparation. Male and female mice aged approximately 8-12 weeks, crossed with a C57BL/6J genetic background, were mainly used for this study. All mice were handled according to the regulations of the Standards for Humane Care and Use of Laboratory Animals of Takasaki University of Health and Welfare and the Guidelines for the Proper Conduct of Animal Experiments from the Ministry of Education, Culture, Sports, Science and Technology (MEXT) of Japan. All animal experiments were approved by the Takasaki University of Health and Welfare Animal Experiment Committee (registration number: 2006, 2038).

### Cell lines

The mouse ES-derived MC-like cell line MEDMC-BRC6, was purchased from RIKEN BioResource Center (BRC, Tsukuba, Japan) and was cultured as described previously (Hiroyama et al., 2008; Shibagaki et al., 2017). Briefly, the cells were cultured in Iscove's modified Dulbecco's medium (IMDM; SIGMA) containing the following: 15% fetal bovine serum (FBS), ITS liquid medium supplement (SIGMA), 50 mg/mL ascorbic acid (SIGMA), 0.45 mM α-monothioglycerol (SIGMA), 3 ng/mL IL-3 (PeproTech), 30 ng/mL stem cell factor (SCF; PeproTech), 1% penicillin–streptomycin solution (Nacalai Tesque), and 2 mM L-glutamine (Nacalai Tesque). P815 cells and MEL cells were cultured as previously described (Minegishi et al., 2005; Ohmori

et al., 2012). Raw264.7 cells were cultured in Dulbecco's Modified Eagle's Medium (DMEM) with high glucose supplemented with 10% FBS.

## METHOD DETAILS

### Peritoneal cell-derived mast cell

Peritoneal cell-derived mast cells (PMCs) were generated as described previously (Malbec et al., 2007). Briefly, mouse peritoneal cells were collected from the peritoneal cavities of 8- to 12-week-old mice and cultured with Roswell Park Memorial Institute (RPMI) 1640 medium (Nacalai Tesque) supplemented with 10% FBS (GIBCO), 1% streptomycin/penicillin (Nacalai Tesque), 10 ng/mL recombinant murine interleukin-3 (IL-3; Peprotech) and 10 ng/mL recombinant murine (Peprotech). On cell culture day 14, when almost all (>95%) cells were positive for c-Kit and FcεRIα as determined by fluorescence-activated cell sorting (FACS), the PMCs were treated with 0.5 μM 4-OHT (Sigma H7904) to induce Cre-mediated recombination. Twenty-four hours after Cre-induction, the PMCs were treated with LPS for 2 hours and subjected to analysis.

### RNA extraction and quantitative real-time RT–PCR (RT–qPCR)

Total RNA was prepared with NucleoSpin RNA Plus (TaKaRa) according to the manufacturer's instructions. The RNA samples were reverse-transcribed using a ReverTra Ace qPCR RT kit (Toyobo) following the manufacturer's instructions. For RT–qPCR, cDNA was analyzed by Thermal Cycler Dice Real-Time System III (TAKARA) with THUNDERBIRD Next SYBR qPCR Mix (TOYOBO) according to the manufacturer's instructions. The data were normalized to *Polr2a* expression levels and are shown as the means ± the standard deviations (SD).

### Transfection of siRNAs

MEDMC-BRC6 cells were resuspended in OPTI-MEM (Invitrogen), and 100 μL of cell suspension at a density of $2 \times 10^4$ cells/μL was mixed with 2 μM siRNA. The cells and siRNA suspension were added to electroporation cuvettes and electroporated in a NEPA21 Super Electroporator (NEPA GENE). Square electric pulses were applied at 200 V (pulse length, 5.0 ms).

### Chromatin immunoprecipitation (ChIP) assay

The ChIP assay and quantitative analysis of DNA purified from the ChIP samples were conducted as described previously (Ohmori et al., 2012; Takai et al., 2013). Briefly, cells were cross-linked with 1% formaldehyde for 10 min and lysed. The samples were sonicated to shear the DNA using a focused ultrasonicator M220 (Covaris) with duty factor 5%, peak incident power 75 W, and 200 cycles per burst for 300 sec. The solubilized chromatin fraction was incubated with the primary antibodies overnight, which were prebound to anti-rabbit IgG-conjugated Dynabeads (for anti-H3K27ac antibody) or anti-mouse IgG conjugated Dynabeads (for the rest of the antibodies) (Thermo Fisher Scientific). The primary antibodies used for the ChIP assay were anti-PU.1 (C-3; Santa Cruz), anti-GATA2 (B9922A; Perseus Proteomics), and anti-H3K27ac (Cat#ab4729, Abcam). The DNA purified from ChIP samples was decrosslinked, purified, and subjected to analysis using a Thermal Cycler Dice Real-Time System III (TAKARA) with THUNDERBIRD Next SYBR qPCR Mix (TOYOBO). The primers used for the ChIP assays are listed in the Key resources table.

### Chromatin immunoprecipitation sequencing

For ChIP-Seq analysis, MEDMC-BRC6 cells were treated with LPS (1 μg/mL 2 hours). Precipitated DNA was decrosslinked, purified with a QIAquick PCR Purification kit (QIAGEN), quantified with a Qubit Fluorometer (Life Technologies) and used for library preparation. Sequencing libraries were prepared from 1.0 ng of ChIPed DNA and input samples using a NEBNext Ultra II DNA Library Prep Kit for Illumina according to the manufacturer's instructions (New England Biolabs). The size distribution of the prepared samples was confirmed to be 300-600 bp using an Agilent 4200 TapeStation (Agilent). Prepared samples were quantified by the quantitative MiSeq (qMiSeq) method (Otsuki et al., 2016), followed by high throughput sequencing using a HiSeq 2500 (Illumina) to generate 101-base single reads.

### Bioinformatics analysis

The sequenced reads were mapped to the mouse genome (mm10) using Bowtie2 software (Langmead and Salzberg, 2012). The mapped tags were visualized by using Integrative Genomics Viewer (Thorvaldsdóttir et al., 2013). Peak calling was performed using a model-based analysis of ChIP-seq (MACS) version 1.4.2

(Zhang et al., 2008). DNA motif construction was performed using HOMER (Hypergeometric Optimization of Motif EnRichment) v4.11 (Heinz et al., 2010; Duttke et al., 2019). Gene ontology analysis was performed using the Genomic Regions Enrichment of Annotations Tool (GREAT) (McLean et al., 2010). Consensus binding sites for transcription factors were predicted by JASPAR (http://jaspar.genereg.net). The data generated in this publication have been deposited in the DNA Database Japan (DDBJ) and are accessible through accession number PRJDB12807. The publicly available ChIP-seq data in mouse BMMCs (for ATAC-seq, SRX2404770; for H3K27ac, SRX1456413; for PU.1, SRX310205; for GATA2, SRX310202) were aligned to the mouse reference genome (mm10) and visualized using the Integrative Genomics Viewer (IGV).

### Preparation of CRISPR–Cas9 ribonucleoprotein (RNP)

Cas9 RNP complexes were prepared by following the manufacturer's protocol. Briefly, Alt-R CRISPR–Cas9 CRISPR RNAs (crRNAs), trans-activating CRISPR RNA (tracrRNA), and Cas9 nuclease V3 were purchased from Integrated DNA Technologies, Inc. The crRNA target sequences were as follows: crRNA1: AGATTATAACAAACGATGGT, crRNA2: GTGGCTGGATTGGCAGAACT. The tracrRNA and one of the crRNAs were mixed and annealed to form a crRNA:tracrRNA duplex (gRNA). The recombinant Cas9 nuclease V3 was mixed with the gRNA solution to form RNP. RNPs were electroporated into BRC6 cells immediately after forming the Cas9 RNP complexes. We obtained ten clones of homozygous deletion, which were examined by quantitative PCR and Sanger sequencing. Eight out of the ten homozygous clones were mixed and subjected to the subsequent analysis.

### QUANTIFICATION AND STATISTICAL ANALYSIS

The data are presented as the mean $\pm$ standard deviation (SD) or mean $\pm$ standard error of the mean (SEM). Unless otherwise specified, comparisons between two groups were performed using an unpaired Student's $t$ test and the Mann–Whitney U test as described in the figure legends. Comparisons among multiple groups were performed using one-way analysis of variance (ANOVA) with Dunnett's test or Tukey's post-hoc test as described in the figure legends. For all of the analyses, statistical significance was defined as a value of *: $p < 0.05$ or **: $p < 0.01$. Data management and statistical analysis were performed using Excel (Microsoft, Redmond, WA), GraphPad Prism 8 software (GraphPad Software, San Diego, CA), or KaleidaGraph Version 4.5 (HULINKS Inc., Tokyo, Japan).